



# Flood risk assessment using geospatial data and multi-criteria decision approach: a study from historically active flood-prone region of Himalayan foothill, India

Subham Roy<sup>1</sup> · Arghadeep Bose<sup>1</sup> · Indrajit Roy Chowdhury<sup>1</sup>

Received: 28 February 2021 / Accepted: 12 May 2021 / Published online: 27 May 2021  
© Saudi Society for Geosciences 2021

## Abstract

In recent years, floods have acquired global importance due to their devastating nature that can cause massive damage to infrastructure and society. The Himalayan foothill is very susceptible to flood since time immemorial, and therefore, the present study tries to assess the flood risk of the sub-Himalayan Jalpaiguri region using a multi-criteria decision approach. Hitherto, a detailed assessment of flood in the Himalayan foothill region is not carried due to a comprehensive database limitation. However, for the first time, a multi-source data of about seventeen parameters including, flood conditioning factors (viz. altitude, distance from rivers, slope, drainage density, geomorphology, flow accumulation, rainfall, topographic wetness index, geology, and soil) and socio-economic and infrastructural indicators (viz. population density, household density, Landcover, road distance, proximity to flood shelter, proximity to hospital and literacy) were used to prepare the flood susceptibility, vulnerability, and flood risk map for the study area. Furthermore, an administrative-wise microlevel risk assessment was also carried out in the present study. The result indicates that about 38% of the area is susceptible to high and very high flood zones, while about 58% of the area is covered under high to very high vulnerability zone. In the final flood risk map, about 29% of the area is under a high threat level that seeks immediate consideration. Furthermore, the reliability of this work can be assessed by validating the model using AUC, which gives an accuracy of 0.862 or 86.2%. Thus, the overall approach of this study can be applied for mitigation strategy and to prepare a policy framework to alleviate future flood incidences.

**Keywords** Flood susceptibility · Flood risk · Flood vulnerability · AHP · Himalaya · India

## Introduction

One of the most devastating natural events is flooding, comprising around one third of all environmental threats (Smith and Ward 1998; Adhikari et al. 2010). Over the last few decades, across the world, floods have drawn sincere attention

from researchers because of their catastrophic character and ability to inflict significant economic casualties and life losses (Kron et al. 2012; Nied et al. 2017). Trends of the flood have increased globally over the past three decades, mainly due to the increasing impacts of climate change, alteration of land use, and other human activities (Kourgialas and Karatzas 2011). About 90% of flood-induced natural disasters and 95% of the resulting losses due to floods are experienced by developing countries, particularly those located on the Asian continent (Gupta et al. 2003).

Since floods are not entirely avoided, it is possible to mitigate their detrimental effects (Khosravi et al. 2019). Thus, potential flood assessment and management is a more practical choice that lays out the evolution of the 'flood risk management approach,' consisting of two fundamental foundations such as flood risk mitigation and flood hazard assessment (Kourgialas and Karatzas 2011; Kazakis et al. 2015). It is impossible to eradicate the absolute risk of flood, but with the utilization of geospatial models, the places under the high

---

Responsible Editor: Biswajeet Pradhan

✉ Subham Roy  
subhamm2@gmail.com

Arghadeep Bose  
arghadeepgeo@gmail.com

Indrajit Roy Chowdhury  
ndrjt.roychowdhury@gmail.com

<sup>1</sup> Department of Geography and Applied Geography, University of North Bengal, Siliguri, West Bengal 734013, India

threat of flood susceptibility can be identified for planning purposes (El-Haddad et al. 2020). A significant number of studies identify the “flood susceptibility map” as an effective preventive tool (Das 2019; Mishra and Sinha 2020). Furthermore, flood vulnerability maps are deemed exceptionally useful for management, preparation, and observation of high-risk areas (Hoque et al. 2019). Numerous environmental variables, such as topography, land use, geology, temperature, and hydrological criteria, need to be considered for preparing flood susceptibility maps, which could influence the outbreak of a flood. This strategy is also known as a multi-criteria decision-making approach (MCDA) that is noteworthy in assessing complicated decision-making systems comprising a broad number of criteria (Khosravi et al. 2019). In recent years, several researchers have widely used various statistical and machine learning methods with remote sensing and GIS to delineate flood susceptible map, such as decision trees models (DT) (Tehrany et al. 2013), frequency ratio (Tehrany et al. 2015a), support vector machine (SVM) (Tehrany et al. 2015b), kernel logistic regression (Hong et al. 2015), bivariate and multivariate statistical models (Youssef et al. 2016), neural fuzzy inference model (Bui et al. 2016), analytical hierarchy process (Das 2019; Mishra and Sinha 2020), analytic network process (Dano et al. 2019), GARP and QUEST machine learning techniques (Darabi et al. 2019), random naive Bayes (Tang et al. 2020), Swarm Optimized Multilayer Neural Network (Ngo et al. 2018), extreme gradient boosting (EGB) (Mirzaei et al. 2020), Machine learning techniques (El-Haddad et al. 2020) and others.

According to numerous literature reviews, there were no universal criteria that specify which model should be used in which situation, as the accuracy of the model depends on various criteria like data availability, precision, and structure of the model (Khosravi et al. 2018). Furthermore, analysis has shown that each model has its own set of benefits and drawbacks. However, de Brito and Evers (2016) reviewed almost 128 papers regarding the MCDM model and found that AHP is the most widespread MCDM method for flood susceptibility modeling. Hence, in this present study, AHP-based MCDM technique was applied to assess the flood risk of the Himalayan foothill region.

In India, the summer monsoon’s unpredictable activity is responsible for the vast number of catastrophic flood events (Dhar and Nandargi 2003). Such floods have caused significant loss to crops, properties, economy and can inflict casualties of life (Vishnu et al. 2019). Moreover, Indian floods are a perpetual natural disaster in monsoon-dominated areas, where much of the annual rainfall happens from June to September. Hence, this Monsoon often considers a concern season for around 32 million citizens in the nation who are subjected to face the annual flood inundation phenomena (Kale 2004).

The question of river flooding is of great concern in the region of the Himalayan foothills due to its historical

relevance; the study region has a special orographic as well as physiographic environment governed by the Himalayas range and also being the lowermost riparian part of the sub-Himalayas where most of the rivers are from a common source (Ghosh and Kar 2018; Chakraborty and Mukhopadhyay 2019). These numerous small to large networks of streams descending from this giant landmass of Himalayas meet at the foothills region to form mighty rivers like Teesta, Mahananda, Torsha, Jaldhaka, Raidak, and Sankosh (Roy 2011; Chakraborty and Datta 2013). All these mighty rivers carried an enormous load in the form of sand, silt, boulder, and gravels, which ultimately gets deposited as a finer particle in the foothill region due to less slopes (in part of Darjeeling, Jalpaiguri, Alipurduar, and Coochbehar district) which form a broad, extensive and monotonous floodplains (Starkel et al. 2008). These flat and extensive floodplain regions are susceptible to inundation regularly; even in a single monsoon season, these areas were prone to flooding many times, hampering the livelihoods of the floodplain dwellers. This background makes it essential for the Jalpaiguri foothill region to recognize and assess the risk of flood by considering flood control elements, i.e., flood susceptibility and vulnerability, as fundamental factors.

Large-scale flooding often occurs in the Himalayan foothill area of Jalpaiguri, resulting in significant socio-economic loss and causing havoc on resources. Although the Himalayan foothills have a high probability and threat of flooding, hitherto no accurate mapping and assessment of flood susceptibility, vulnerability, or risk have been done so far. Therefore the significant contributions of this study are (a) to prepare the flood susceptibility, vulnerability, and risk map for data lacking flood-prone Jalpaiguri foothill region, (b) Micro-level (administrative block-wise) assessment of areas under the high threat of flooding for a better mitigation plan. The results of this study are expected to contribute significantly to the literature on flood risk assessment. Also, the outcomes could be beneficial for the decision-makers and bureaucrats for future flood management practices in flood-prone areas over the world.

## Study area

Jalpaiguri district is one of the major regions of Himalayan foothills located at the southern flank of Sub-Himalayas and occupies about 3386.18 km<sup>2</sup>. Geographically, it is extended between 26° 15' 47" N to 26° 59' 34" N and 88° 23' 2" E to 88° 7' 30" E longitude (Fig. 1). Darjeeling and Bhutan bound the district in the north, Alipurduar district in the east, Coochbehar and Bangladesh in the south, and Darjeeling and Bangladesh in the west. The total population of the study area is about 2381596, which is distributed over 7 Community Development blocks, namely, Jalpaiguri Sadar, Maynaguri,



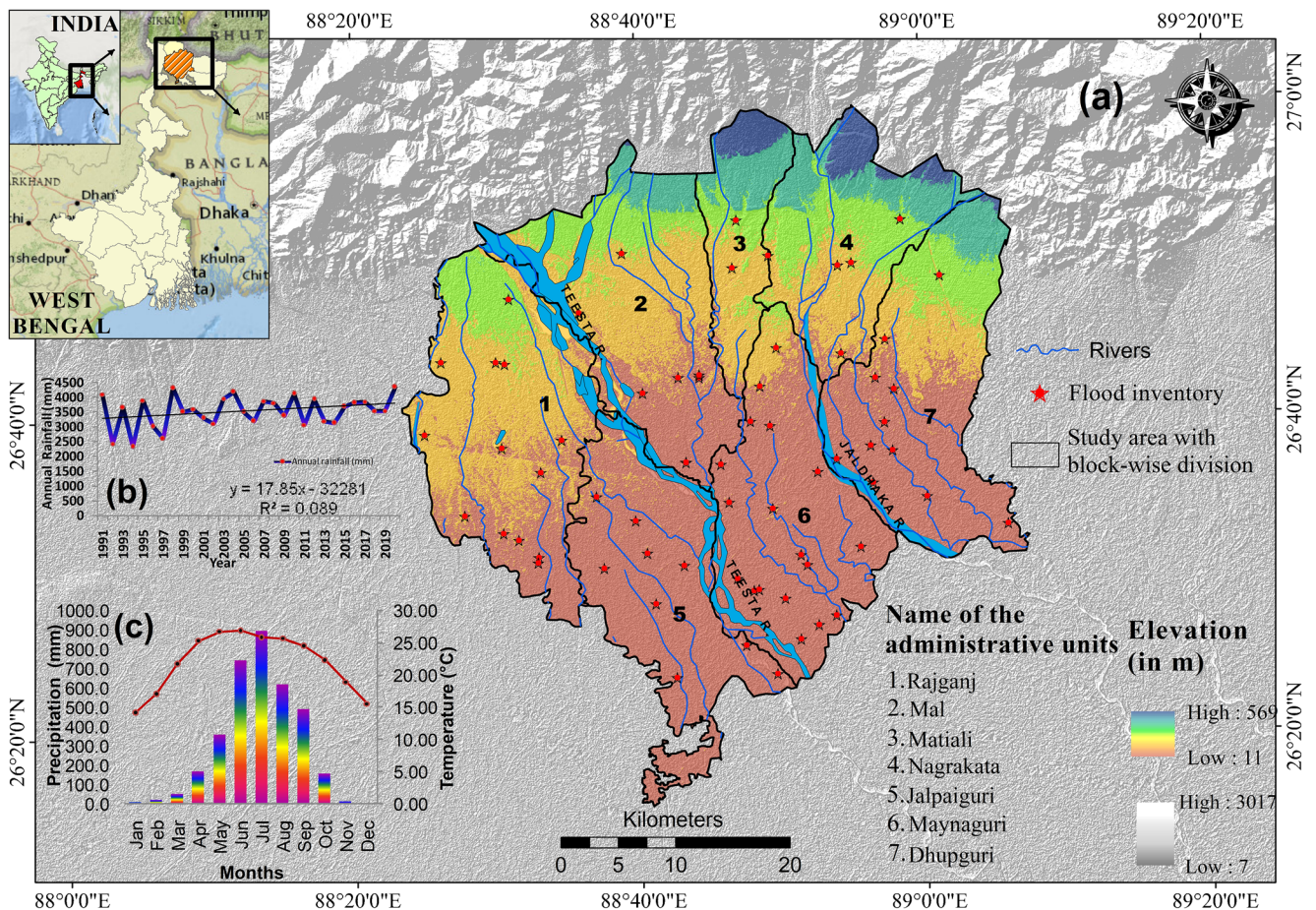


**Fig. 1** (a) Location map of the Jalpaiguri foothill region (study area with administrative boundaries) reference to West Bengal state and India. The map also represents maximum-minimum altitude, major rivers and flood

inventory points (star symbol). (b) Trend of total annual rainfall variability (1991–2020) (Source: [indiawris.gov.in](http://indiawris.gov.in)). (c) Ombrothermic diagram of the study area (mean monthly temperature and rainfall 1991–2019)

Rajganj, Dhupguri, Mal, Nagrakata and Matiali (District Census Handbook, Jalpaiguri 2011, [www.jalpaiguri.gov.in/district-profile](http://www.jalpaiguri.gov.in/district-profile)).

The study area is a vast flat rolling plain in the south with slightly undulating terrain in the north covered with tea gardens and scattered forests. According to the study area's prepared DEM (Fig. 1), the altitude varies from 11 to 569m, and the entire topography is crisscrossed with numerous rivers and streams. Jalpaiguri district is veined by numerous mighty rivers, namely Teesta, Jaldhaka, Mahananda, Daina and others. Climatically, the region experiences a southwest monsoon with high humidity and heavy rainfall. The hot season mainly prevails from March to May, followed by the onset of monsoon from June and continues till October. Further, November to February are the coldest and driest month (District Census Handbook, Jalpaiguri 2011). Besides, the study area's economy is mainly dependent on agriculture and forestry as the majority of the people are engaged in plantation activities, commercial cultivation, and trade and commerce activity (Ghosh and Ghosal 2020).

## History and reason of catastrophic floods in the Jalpaiguri district of Himalayan foothills

The study area is highly susceptible to flood due to its varying climatic nature and high annual rainfall and thus selected for the present study (Roy 2011; Shrestha et al. 2012, 2015; Mandal and Sarkar 2016). The flood impacts in the district are a yearly and common phenomenon, but its intensity might vary. This intensity of flood magnitude may vary in terms of areas inundated, the number of population affected, livelihood and infrastructure damages (Das et al. 2017). All the administrative blocks of Jalpaiguri district are more or less affected by the flood every year. There are three main reasons considered for the flood in the sub-Himalayan Jalpaiguri region, i.e., (i) high-intensity rainfall for short durations on small catchments, (ii) incessant rainfall for several days on bigger catchment and, (iii) as the district situated in the Himalayan foothills thus includes a copious network of rivers and streams which triggers the floods (District Census Handbook 2011;

Chakraborty and Datta 2013). However, not all the flood events were disastrous and widespread; instead, some are purely local, but some are genuinely catastrophic (Chakraborty 2017). Therefore, the occurrences, triggering mechanism, and consequence of some significant catastrophic historical flood of 233 years for Jalpaiguri district are summarized in Table 1.

## Data and methodology

### Data source and preparation technique of thematic layers

The data source and methodological flow chart for the present study have been summarized and given in Table 2 and Fig. 2,

respectively. In order to assess the flood risk of the sub-Himalayan Jalpaiguri district, a total of seventeen thematic layers were selected after extensive literature review and expert opinions. Among these layers, ten parameters are related to flood conditioning or susceptibility factors viz. elevation, slope, drainage density, distance to rivers, geomorphology, rainfall, flow accumulation, topographic wetness index (TWI), geology, and soil. Subsequently, the remaining seven layers are related to flood vulnerability factors, i.e., population density, household density, Landuse, distance to major roads, distance to flood shelter, distance to hospital, and literacy rate. All the layers have been generated in the GIS environment based on in-depth investigation and field observation.

ASTER Global Digital Elevation Model (GDEM) was acquired from NASA with a 30-m resolution to prepare elevation, slope, drainage density, flow accumulation, and TWI.

**Table 1** Synopsis of some major historical floods occurred in Himalayan foothill region of Jalpaiguri district, India

Year	Causes	Affected areas	Reference
1787	Triggered by earthquake and heavy rainfall	Large part of Jalpaiguri, coochbehar and Darjeeling. Tista river shifted its course from Ganga to Brahmaputra	Mahalanobis (1927), Roy (2011)
1840	Heavy rainfall	Jalpaiguri, coochbehar and Darjeeling district. Sankosh and Torsa river shifted their course	Mahalanobis (1927), Roy (2011)
1892	Extreme rainfall	Jalpaiguri and adjoining district. Jaldhaka river shifted its course	Mahalanobis (1927), Roy (2011)
1906	Incessant rainfall of about more than 1000mm in 72 h	Jalpaiguri and adjoining district. There was huge damage to land and property	Mahalanobis (1927), Roy (2011)
1950	Extreme rainfall in catchment area of Tista, Jaldhaka and Mahananda rivers	There was huge damage to land, animals, human lives and food crops in the entire foothill region	Roy (2011)
1968	Cloud-brust over Himalayan foothill region with 1200mm rainfall which trigger huge landslide and damming of river	The most devastating flood of the region. Jalpaiguri was worst affected part with 217 people death, 3456 damaged house and 1360 died cows. Also huge damage occurred to communication lines, land and property	Roy (2011), Ghosh and Ghosal (2020), <a href="http://www.anandabazar.com/editorial/50-years-of-devastating-flood-at-jalpaiguri-1-891083">www.anandabazar.com/editorial/50-years-of-devastating-flood-at-jalpaiguri-1-891083</a>
1998	Cloud-brust over the Bhutan hills with 1250mm in 72 h	Foothill region was severely damaged and Jalpaiguri was most affected. Also many rivers shift it course, tea gardens, forest and settlement was destructed	Roy (2011)
2003	Heavy rainfall	About 30000 people of Jalpaiguri were affected, with 500 acres damaged tea garden and missing of about 215 meters long embankment	Roy (2011), Ghosh and Ghosal (2020)
2007	Excessive rainfall of about 350mm in 24 h due to cloud-brust with	Affecting 25000 families in Jalpaiguri with 6500 houses got annihilated and about 4500 hectare of arable land was destroyed	Roy (2011), Ghosh and Ghosal (2020)
2009	Heavy rainfall	Jalpaiguri, Mal and Maynaguri were severely affected. 2 died and 25000 families were abandoned	Roy (2011), Ghosh and Ghosal (2020)
2015	Heavy rainfall	Around 400 people are affected. Rajganj block are severely flooded	The economic times (2015)
2016	Heavy rainfall	Around 150 villages were inundated and 58000 peoples are affected over North Bengal. Jalpaiguri is most affected	Hindustan times (2016)
2017	Heavy rainfall	Villages of Dhupguri, Maynaguri and Mal of Jalpaiguri were inundated. Around 60000 people are severely affected	The Indian express (2016)
2020	Incessant rain	Mal block of Jalpaiguri was severely affected. Many houses, transport lines and cultivable land of Jalpaiguri were submerged	Telegraph (2020)



**Table 2** Thematic layers used for Flood risk assessment, their sources and details

Sl. No	Parameters	Data types	Data details	Source
<b>Flood susceptibility parameter</b>				
1	Elevation	ASTER GDEM	Version 3, 30m × 30m	<a href="https://search.earthdata.nasa.gov">https://search.earthdata.nasa.gov</a>
2	Slope	ASTER GDEM	Version 3, 30m × 30m	<a href="https://search.earthdata.nasa.gov">https://search.earthdata.nasa.gov</a>
3	Drainage density	ASTER GDEM	Version 3, 30m × 30m	<a href="https://search.earthdata.nasa.gov">https://search.earthdata.nasa.gov</a>
4	Flow accumulation	ASTER GDEM	Version 3, 30m × 30m	<a href="https://search.earthdata.nasa.gov">https://search.earthdata.nasa.gov</a>
5	Topographic wetness index	ASTER GDEM	Version 3, 30m × 30m	<a href="https://search.earthdata.nasa.gov">https://search.earthdata.nasa.gov</a>
6	Geomorphology	Vector layer	Geological survey of India (GSI) data, 1:1091958	<a href="https://www.gsi.gov.in">https://www.gsi.gov.in</a>
7	Distance to Rivers	Vector layer	Geological survey of India (GSI) data, 1:1091958	<a href="https://www.gsi.gov.in">https://www.gsi.gov.in</a>
8	Rainfall	High-resolution gridded data, 0.5° x 0.5°	CRU TS v. 4.04 (Climatic Research Unit gridded Time Series) version 4	<a href="https://sites.uea.ac.uk/cru/data">https://sites.uea.ac.uk/cru/data</a>
9	Geology	Shape file	U.S. Geological Survey, Version 2.0	<a href="https://certmapper.cr.usgs.gov/data/apps/world-maps/">https://certmapper.cr.usgs.gov/data/apps/world-maps/</a>
10	Soil	ESRI shapefile	Digital Soil Map of the World (DSMW), FAO	<a href="http://www.fao.org/geonetwork/srv/en/">http://www.fao.org/geonetwork/srv/en/</a>
<b>Flood vulnerability parameter</b>				
1	Population density	Attribute data	District census hand book, Census of India, 2011	<a href="https://censusindia.gov.in/2011census/">https://censusindia.gov.in/2011census/</a>
2	Household density	Attribute data	District census hand book, Census of India, 2011	<a href="https://censusindia.gov.in/2011census/">https://censusindia.gov.in/2011census/</a>
3	Literacy rate	Attribute data	District census hand book, Census of India, 2011	<a href="https://censusindia.gov.in/2011census/">https://censusindia.gov.in/2011census/</a>
4	Land use	Landsat 8 OLI/TIRS	USGS, 30m x 30-m	<a href="https://earthexplorer.usgs.gov">https://earthexplorer.usgs.gov</a>
5	Distance to flood shelter	Location of rescue shelter	District Disaster Management Plan, Jalpaiguri, 2020	<a href="http://www.jalpaiguri.gov.in/">http://www.jalpaiguri.gov.in/</a>
6	Distance to hospital	Location of hospitals	Google maps	<a href="https://www.google.com/maps/">https://www.google.com/maps/</a>
7	Distance to road	Road network shape file	Open Street Map Data	<a href="https://www.openstreetmap.org/">https://www.openstreetmap.org/</a>
*	<b>Flood inventory</b>	Location of flooded area	Sites identification from field investigation, Annual flood report of Jalpaiguri district (1995–2018) ( <a href="http://www.wbiwd.gov.in">www.wbiwd.gov.in</a> ), Bhuvan ISRO ( <a href="http://www.bhuvan-app1.nrsc.gov.in/nfvas/#">www.bhuvan-app1.nrsc.gov.in/nfvas/#</a> ) unpublished reports and newspapers	

First, DEM was pre-processed in the GIS environment using sink-filling, flow accumulation, and flow direction techniques by adopting the hydrology tool. After that, the line density tool was used to prepare the drainage density map. For TWI preparation, the techniques like upslope contributing area (a), slope raster, and a raster calculator in ArcGIS. Subsequently, data were collected from the Bhukosh server of the Geological Survey of India (GSI) for the preparation of geomorphology and distance to rivers. These data are available in vector format, which is processed GIS environment and converted into a raster layer. To represent the geological variation, USGS world geological map, which is available in a shapefile, was clipped for the study area. Subsequently, Rainfall data were obtained from a high resolution of 0.5° × 0.5° CRU (Climatic Research Unit) web satellite and extracted for the study area for the year 2011–2019. For the preparation of the final rainfall map, the Kriging interpolation technique was adopted.

According to many reports, the Kriging interpolation method seems more precise and effective than any other technique for delineating rainfall maps (Kim et al. 2011; Ly et al. 2013). Further, FAO-Digital Soil Map of the World (DSMW) was used to prepare the study area's soil map. All these layers are prepared to fulfill the susceptibility indicators of Jalpaiguri sub-Himalayan region.

Furthermore, to assess the vulnerability indicators, a set of demographic data were used viz., Population density, household density, and literacy rate, extracted from the District Census Handbook (DCHB) of Jalpaiguri district, Census of India, 2011. All these data are incorporated in the attribute tables of the GIS environment to prepare the final thematic layers. Landsat 8 OLI (30-m resolution) imagery was collected from Earth Explorer, US Geological Survey website for the Landcover map preparation. At first, two Landsat images (Row 41, 42 and Path 139) were mosaic, which was later

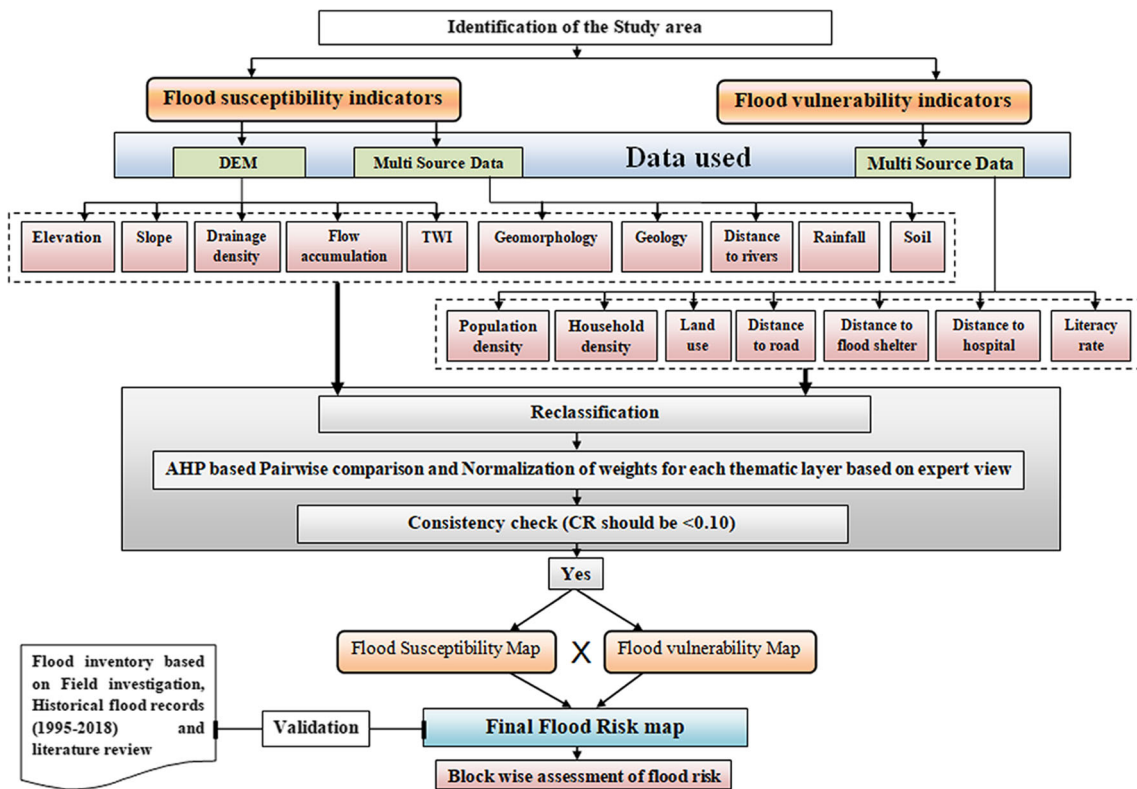


Fig. 2 Methodological flowchart applied for the present study

pre-processed using atmospheric correction, edge enhancement, and band composition. Finally, supervised classification with a maximum likelihood algorithm was performed to generate the final LULC map with respective classes. Distance from the flood shelter map was prepared using multi-buffer points and the coordinates of these flood relief shelters are available in the District Disaster Management Plan of Jalpaiguri district (2016–2020). Similarly, for distance to hospital, Google maps were used to mark the coordinates and later prepared using multi-buffer points in the GIS suite. Lastly, an openstreet server was used to prepare the thematic layer of distance to major roads.

Hence, it is clear that several multi-source data are required to achieve the final outcome in this study, summarized in Table 2. After preparing all the thematic layers, it is rasterized and converted into UTM Projection, Zone 45N, WGS-84 Datum with the same cell size of 30-m spatial resolution. Subsequently, reclassification was done and the weight assigned to each parameter based on the analytical hierarchy process (AHP) technique.

### Multi-criteria decision-based AHP model for weight assignment and normalization

According to (Sener et al. 2011), AHP is a comprehensive technique that incorporates practical knowledge and

subjective ideas to determine the decision-making by assessing multiple variables based on expert opinions using the GIS environment. AHP is introduced by (Saaty 1980, 1990), is an effective decision-making approach based on a set of indicators to create a hierarchical structure by assigning weights to each criterion to reduce the complication in decision-making. Saaty’s AHP offers a method for resolving a variety of decision-making problems based on the relative importance of each criterion for achieving a specific goal (Handfield et al. 2002). According to Pourghasemi et al. (2012), it is a powerful instrument in the discipline of hazard management as it considers multiple parameters for the assessment and later converted each into scores for efficient judgment.

In the present study, the AHP model is used to assign the weights of both susceptibility and vulnerability indicators. However, there are several weight estimation techniques, but among all these, AHP is considered as a promising technique in flood risk assessment that can produce rapid, most reliable and cost-effective performance (Ghosh and Kar 2018; Souissi et al. 2019; Hammami et al. 2019; Dano et al. 2019; Saha and Agrawal 2020; Das 2020). The assigning of weights to each parameter and their normalization is a critical consideration to produce reliable outcomes since the final result relies entirely on the assignment of suitable weights (Muralitharan and Palanivel 2015). In order to compare all parameters of the thematic layer against each other in a matrix format which is

useful in the deriving calculation, the weights of each criterion were allocated based on Saaty’s scale (1–9) of relative importance (Table 3). The Saaty scale of importance indicates “9” with “extreme importance” and “1” with “equal importance” (Table 3). The AHP model consists of four stages, viz. (i) weight assignment, (ii) pairwise comparison matrix, (iii) weight normalization, and (iv) consistency check (Benjmel et al. 2020; Ghosh et al. 2020). All the seventeen parameter’s weight is assigned based on several expert opinions, field knowledge, and numerous literature reviews (Ghosh and Kar 2018; Souissi et al. 2019; Das 2019; Chakraborty and Mukhopadhyay 2019; Khosravi et al. 2019; Saha and Agrawal 2020).

The following steps are adopted to compute Pairwise comparison matrix and to check the consistency (Arefin 2020).

Step 1: Pairwise comparison matrix (PCM) calculated using Eq. 1

$$X = \begin{bmatrix} X_{11} & X_{12} & \dots & X_{1n} \\ X_{21} & X_{22} & \dots & X_{2n} \\ \dots & \dots & \dots & \dots \\ X_{n1} & X_{n2} & \dots & X_{nn} \end{bmatrix} \tag{1}$$

where  $X$  is the Pairwise comparison matrix,  $X_{nn}$  is the indicator of Pairwise matrix element.

Step 2: Normalization of the weights using Eq. 2

$$NW = \left( \frac{GM}{\sum_{n=1}^n GM_n} \right) \tag{2}$$

where  $NW$  is normalized weights,  $GM_n$  is consider as Geometric mean of  $n$ th row of Pairwise matrix ( $X$ ).

Furthermore,  $GM_n$  can be expressed as Eq. 3

$$GM_n = \sqrt[n]{X_{1n}X_{2n}\dots X_{nn}} \tag{3}$$

Step 3: The Consistency ratio (CR) is used to validate the AHP judgment coherence using Eq. 4 (Saaty 1980)

$$CR = \frac{CI}{RI} \tag{4}$$

where CR is calculated dividing CI (Consistency index) by RCI (Random consistency index) of Saaty (Table 3).

Saaty (1980) presented random index (RI) values used to measure the consistency of the Pairwise comparison matrix. According to the ten selected parameters in this study for the flood susceptibility model, the random index is 1.49. Consequently, for the vulnerability model, seven parameters were selected, with the RI value of 1.32. Based on Saaty (1990), the CR value of less than 0.10 is acceptable to continue the analysis. However, in our study, the CR value is less than 0.10 for both susceptibility and vulnerability indicators (Tables 4 and 6), and hence, it is adequate to continue the analysis. Otherwise, if the CR value is more than 0.10, it is necessary to modify the analysis from the beginning to determine the source of inconsistency in the matrix (Saaty 1977).

Step 4: To calculate CI, the Eq. 5 was adopted

$$CI = \frac{(\lambda_{max}-n)}{(n-1)} \tag{5}$$

where  $\lambda_{max}$  is the principle Eigen value, and  $n$  indicates the total number of parameters selected for study.

### Delineation of Flood susceptibility and vulnerability map

After priority-based normalization, the relative weights of each parameter were used to measure the flood susceptibility index (FSI) and flood vulnerability index (FVI) in the ArcGIS setting, which was calculated by multiplying the sum of weights by the rate of each factor. The following equations are used to model the FSI and FVI (Das 2018, 2020;

**Table 3** Relative importance scale (1–9) and Random consistency index (RCI) based on Saaty (1980, 1990)

Intensity of Importance	1	2	3	4	5	6	7	8	9	-
Definition	Equal	Weak	Moderate	Moderate plus	Strong	Strong plus	Very strong	Very very strong	Extreme	-
n (No. of parameters selected)	1	2	3	4	5	6	7	8	9	10
RCI value	0	0	0.58	0.90	1.12	1.24	1.32	1.41	1.45	1.49



**Table 4** Pairwise comparison matrix for flood susceptibility parameters and their normalized weights based on Saaty’s AHP

	EL	SL	DR	DD	GM	RF	FA	TWI	GL	SOIL	Geometric Mean	AHP normalized weight
EL	9/9	9/8	9/7	9/7	9/6	9/6	9/5	9/5	9/4	9/3	1.57	0.15
SL	8/9	8/8	8/7	8/7	8/6	8/6	8/5	8/5	8/4	8/3	1.41	0.13
DR	7/9	7/8	7/7	7/7	7/6	7/6	7/5	7/5	7/4	7/3	1.25	0.12
DD	7/9	7/8	7/7	7/7	7/6	7/6	7/5	7/5	7/4	7/3	1.22	0.12
GM	6/9	6/8	6/7	6/7	6/6	6/6	6/5	6/5	6/4	6/3	1.05	0.10
RF	6/9	6/8	6/7	6/7	6/6	6/6	6/5	6/5	6/4	6/3	1.05	0.10
FA	5/9	5/8	5/7	5/7	5/6	5/6	5/5	5/5	5/4	5/3	0.87	0.08
TWI	5/9	5/8	5/7	5/7	5/6	5/6	5/5	5/5	5/4	5/3	0.87	0.08
GL	4/9	4/8	4/7	4/7	4/6	4/6	4/5	4/5	4/4	4/3	0.70	0.07
SOIL	3/9	3/8	3/7	3/7	3/6	3/6	3/5	3/5	3/4	3/3	0.52	0.05
Column Total											10.52	1.00

EL= elevation, SL= slope, DR= distance to river, DD= drainage density, GM= geomorphology, RF= rainfall, FA= flow accumulation, TWI= topographic wetness index, GL= geology

Maximum eigenvalue ( $\lambda_{max}$ ) = 10.041, CI= 0.00453, n =10, RI= 1.49, CR= 0.0030

Kittipongvises et al. 2020; Malik et al. 2020).

$$FSI = \sum_{i=1}^n W_i^F \times R_i^F \tag{6}$$

$$FVI = \sum_{i=1}^n W_i^V \times R_i^V \tag{7}$$

where FSI and FVI are flood susceptibility index and flood vulnerability index,  $n$  is the numbers of factors,  $W_i$  is the weights of each susceptibility parameter, and  $R_i$  is the rank of each parameters.

### Preparation of flood risk map

Flood risk assessment is a crucial task to mitigate and manage floods, especially in flood plain areas, including geo-environmental hazards and socio-economic factors. According to Merlotto et al. (2016), the number of lives lost, people injured, property damaged, and the overall adverse effects on economic growth due to natural disasters is referred to as the cumulative risk assessment. It is a product of the possibility of a site experiencing regular flood events and the degree of instability of the system. Therefore risk can be measured as a cross-cutting mix of hazard and vulnerability.

Thus, flood risk mapping of the entire sub-Himalayan Jalpaiguri district has been calculated by multiplying the final susceptibility index and vulnerability index using the following equation in the raster calculator (Danumah et al. 2016; Ghosh and Kar 2018; Chakraborty and Mukhopadhyay 2019; Das 2020).

$$Flood\ risk\ index = FSI \times FVI \tag{8}$$

### Flood inventory

A flood inventory map displays detailed positions of areas inundated based on historical flooding records and can also predict future flood events of specific locations (Rahmati et al. 2016; Souissi et al. 2019). Therefore, it is the most vital part and an essential requirement for any susceptibility and vulnerability mapping. A flood inventory map can be prepared using several methods that depend on various conditions like the motive of the study, data availability, records of historical flood incidents, interpretation of satellite images, and access to geo-environmental conditions (Arabameri et al. 2019; Chen et al. 2019; Khosravi et al. 2019).

Thus for the present study of the Jalpaiguri district, about 68 locations were identified for flood inventory mapping. These points are selected and identified after extensive field exploration using Google maps GPS and historical flood record from (1995 to 2018) available from the Irrigation and Waterways Department, Government of West Bengal ([www.wbiwd.gov.in/](http://www.wbiwd.gov.in/)). Also, several newspapers, unpublished work and the Bhuvan portal of ISRO (<https://bhuvan-app1.nrsc.gov.in/nfvas/#>) are used to cross-validate the flood inventory points.

### Flood conditioning factors

According to several experts opinions and literature review (Sharma et al. 2017; Danumah et al. 2016; Hu et al. 2017; Hazarika et al. 2018; Ghosh and Kar 2018; Chakraborty and Mukhopadhyay 2019; Das 2019; El-Haddad et al. 2020), a total of about ten thematic layers were selected (Table 5 and

**Table 5** Sub-criteria of selected susceptibility parameters with their assigned and normalized ranks

Parameters	Normalized AHP weights	Sub-classes	Rank	Normalized Rank
Elevation	0.15	11–92	5	0.33
		92–136	4	0.27
		136–198	3	0.20
		198–293	2	0.13
		293–596	1	0.07
Slope	0.13	0–3.04	5	0.33
		3.04–5.90	4	0.27
		5.90–9.52	3	0.20
		9.52–15.62	2	0.13
		15.62–48.58	1	0.07
Distance from rivers	0.12	<250	5	0.33
		250–500	4	0.27
		500–1000	3	0.20
		1000–1500	2	0.13
		>1500	1	0.07
Drainage density	0.12	0–0.15	1	0.07
		0.15–0.33	2	0.13
		0.33–0.52	3	0.20
		0.52–0.72	4	0.27
		0.72–1.25	5	0.33
Geomorphology	0.10	Active flood plain	5	0.23
		Older flood plain	5	0.23
		Piedmont alluvial plain	4	0.18
		Younger alluvial plain	4	0.18
		Water bodies	3	0.14
		Hills and valleys	1	0.05
Rainfall	0.10	2013–2102	2	0.13
		2102–2164	2	0.13
		2164–2222	3	0.19
		2222–2288	4	0.25
		2288–2388	5	0.31
Flow accumulation	0.08	0–37080	1	0.07
		37080–142141	2	0.13
		142141–346084	3	0.20
		346084–821951	4	0.27
		821951–1575922	5	0.33
TWI	0.08	3.40–6.47	1	0.07
		6.47–8.04	2	0.13
		8.04–10.11	3	0.20
		10.11–13.18	4	0.27
		13.18–24.53	5	0.33
Geology	0.07	Quaternary sediments	4	0.40
		Neo. sedimentary origin	3	0.30
		Ud. Precambrian rocks	2	0.20
		Ud. Paleozoic rocks	1	0.10

**Table 5** (continued)

Parameters	Normalized AHP weights	Sub-classes	Rank	Normalized Rank
Soil	0.05	Fine coarse loam	4	0.21
		Coarse loam	3	0.16
		Loam	3	0.16
		Fine sandy loam	2	0.11
		Sandy loam	2	0.11
		Clay	1	0.26

Fig. 2). Therefore, these selected indicators can be considered as a flood-determining factor for the Jalpaiguri foothill region.

**Elevation**

Water flows smoothly from upland to lowland regions because of the gravity influence, while the water across the lower elevated plains remains stagnant for a more extended period which induces floods (Tehrany et al. 2014; Das 2019). In the study area, the elevation can be categorized into five classes, i.e., flat (11–92), gentle (92–136), moderate (136–198), steep (198–293), very steep (293–569) (Fig. 3a) (Table 6).

**Slope**

The topographic slope usually limits water velocity and act as a flood controlling factors. Besides, the topographic gradient has considerable influence over the infiltration rate (Das 2019). Therefore, a huge volume of water becomes sluggish near the sites of low lying flat topography and thus, low geographic slope usually displays greater susceptibility to flood (Bui et al. 2019). In the study area, the slope is categorized into five zones, i.e., flat (0°–3°), gentle (3°–6°), sloping (6°–10°), steep (10°–16°), very steep (>15°) (Fig. 3b).

**Distance from rivers**

Distance from rivers is another significant factor that plays a vital role in determining flood conditions. According to several researchers (Rahmati et al. 2016; Ghosh and Kar 2018; Bui et al. 2019) flooding is expected in the areas near the river due to heavy runoff in the drainage system, mainly after intense rainfall, which consequences in exceeding the limit of stream capacity. However, there is no common opinion regarding the distance that may provide a higher susceptibility, as small waterways can be flooded up to several meters while large rivers can cross several kilometers since the distance varies from river to river. Pradhan (2009) observed that areas proximate to 90 m from rivers are more susceptible, while Samanta et al. (2016) consider less than 100m distances are more vulnerable to flood. Therefore, for the present study, five consecutive classes range from less than 250m to above 1500m were prepared (Fig. 3c).

**Drainage density**

Horton (1945) described drainage density as the ratio of the total length of channel segments for all stream order in a basin area, and this parameter is considered one of the significant attributes of landscapes that have formed under the fluvial effect. The greater the drainage intensity indicates a greater

**Table 6** Pairwise comparison matrix for flood vulnerability parameters and their normalized weights based on Saaty’s AHP

	PD	HD	LULC	DR	DFS	DH	LR	Geometric Mean	AHP normalized weight
PD	9/9	9/8	9/7	9/6	9/6	9/5	9/4	1.45	0.20
HD	8/9	8/8	8/7	8/6	8/6	9/5	8/4	1.31	0.18
LULC	7/9	7/8	7/7	7/6	7/6	7/5	7/4	1.12	0.16
DR	6/9	6/8	6/7	6/6	6/6	6/5	6/4	0.96	0.13
DFS	6/9	6/8	6/7	6/6	6/6	6/5	6/4	0.96	0.13
DH	5/9	5/8	5/7	5/6	5/6	5/5	5/4	0.80	0.11
LR	4/9	4/8	4/7	4/6	4/6	4/5	4/4	0.64	0.09
Column Total								7.25	1.00

PD= population density, HD= household density, LULC= land use, DR= distance to road, DFS= distance to flood shelter, DH= distance to hospital, LR= literacy rate

Maximum eigenvalue ( $\lambda_{max}$ ) = 7.0178, CI= 0.00296, n =7, RI= 1.32, CR= 0.0024



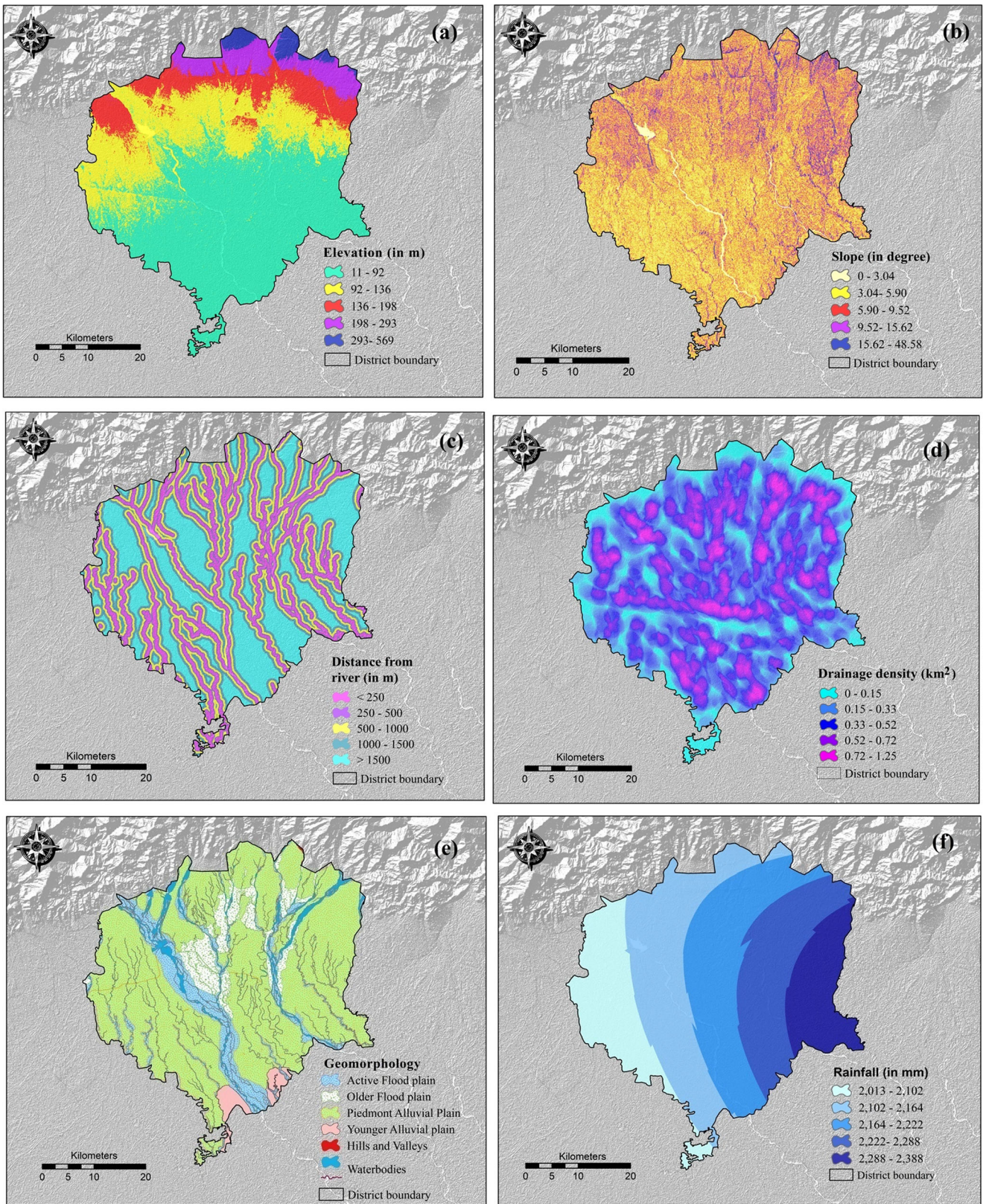


**Fig. 3** Flood conditioning indicators (a) elevation, (b) slope, (c) distance from rivers, (d) drainage density, (e) geomorphology, (f) rainfall, (g) flow accumulation, (h) topographic wetness index, (i) geology, and (j) soil



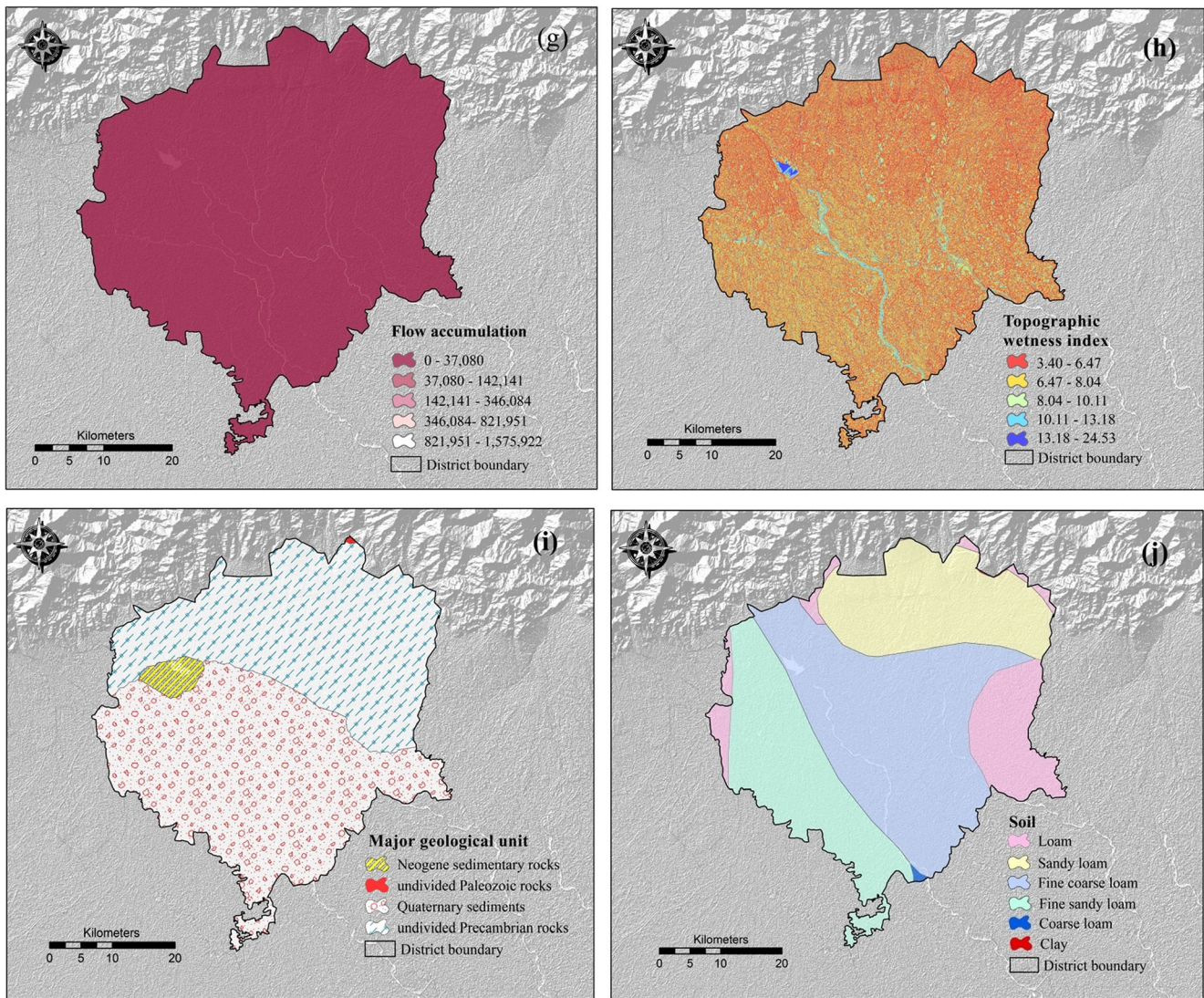


Fig. 3 continued.

length of drainage lines per region of the unit. Therefore, owing to higher drainage density, areas with a dense stream network typically show regular flooding (Ogden et al. 2011; Mirzaei et al. 2020). Figure 3d shows that the Jalpaiguri foothill region shows an intense network of drainage density, and it can be classified into five classes.

### Geomorphology

The geomorphic composition of any area has a significant role in flood conditioning; thus, the sub-Himalayan Jalpaiguri's geomorphology is very important to understand for demarcating flood susceptibility. According to Das (2019), low-lying flood plain regions are more susceptible to flood compared to undulating hilly terrain. However, according to the prepared geomorphology map of the study area (Fig. 3e), it is clear that the Jalpaiguri district is highly susceptible to flood risk as it

mainly comprises a flood plain, alluvial plain, and water bodies.

### Rainfall

The intensity and duration of rainfall directly determine the flood occurrences, as maximum rainfall increases flood hazard risk (Rozalis et al. 2010; Zhao et al. 2018; Mirzaei et al. 2020). The rainfall pattern of the Jalpaiguri foothill area is influenced by the southwest monsoon, and it receives high annual rainfall with regular heavy rains, mainly between June and September (monsoon period). The southern front of the Himalayan ranges acts as a first orographic barrier for S-W monsoon winds, which arrive from the Bay of Bengal to the Himalaya, resulting in a high rainfall during the monsoon season (Prokop and Walanus 2017). Therefore, rainfall plays a vital role that triggers flood incidence in the study area, and

according to the prepared rainfall map (Fig. 3f), the eastern part of the region experiences slightly more rainfall than the western part.

### Flow accumulation

For the assessment of flood and other hydrological factors, flow accumulation is one of the most vital parameters (Kazakis et al. 2015; Das 2020). It can be considered as total flow to a particular point within the catchment from upstream areas and thus, higher flow accumulation indicates a high possibility of flooding. According to the prepared map of the Jalpaiguri foothill (Fig. 3g), the flow accumulation above 821951 can be considered as high susceptible zone, which is concentrated mainly near the river banks.

### Topographic wetness index

The topographic wetness index (TWI), also known as Compound Topographic Index (CTI), refers to the spatial distribution of wetness and regulates overland water flow (Samanta et al. 2018; Ali et al. 2019). According to Das (2020), TWI is a significant parameter that conveys essential knowledge regarding hydro-geomorphological regulation of the landscape. Many researchers often use TWI for flood susceptibility mapping because it determines the area of flood inundation, and the higher the TWI indicates a higher risk of the flood (Bui et al. 2018). TWI for the present study (Fig. 3h) can be prepared using the following equation given by Moore et al. (1991).

$$TWI = \ln \left( \frac{A_s}{\tan\beta} \right) \quad (9)$$

where  $A_s$  is the flow accumulation and  $\tan\beta$  is the surface slope gradient.

### Geology

There is a close link between local geology and flood events because it influences permeability, porosity, and infiltration rates since impermeable rock ameliorate surface runoff, which triggers flooding (Kazakis et al. 2015; Das 2019). Moreover, previous studies find flood susceptibility can be understood by assessing geology as it determines the nature of runoff, influences drainage network, and controls the hydrology (Reneau 2000; Malik et al. 2020; El-Magd et al. 2021). According to the prepared geological map of Jalpaiguri (Fig. 3i), it can be divided into (i) Quaternary sediments, (ii) Neogene sedimentary origin, (iii) undivided Paleozoic origin, and (iv) Precambrian rocks.

### Soil

The soil type of a particular area largely determines the absorption capacity and intensity of runoff which eventually controls flood levels (Souissi et al. 2019; Malik et al. 2020). For example, fine-particle soil, such as silt and clay, has an inadequate transmission capacity and permeability, resulting in high runoff that eventually triggers flood susceptibility (Arya and Singh 2021). In contrast, sandy soil with large pore space increases infiltration and reduces surface runoff (Ibrahim-Bathis and Ahmed 2016; Das 2019, 2020). However, according to Fig. 3j, there are six major types of soil found in the study area.

### Flood vulnerability factors

Merlotto et al. (2016) define vulnerability assessment as the extent and severity of damage to a specific component due to natural phenomena. In specific, the evaluation of vulnerability contains an integrated system of risk factors that can cause catastrophic to human beings, loss of property, disruption of the social system, setback of wealth and resources (Balica et al. 2012; Ghosh 2016). Thus, flood vulnerability indicates the amount and extent of harm under specific socio-economic conditions and resilience capacity for a particular area in the present context. However, the present study's vulnerability parameters were chosen after an extensive literature review (Hu et al. 2017; Danumah et al. 2016; Ghosh and Kar 2018; Chakraborty and Mukhopadhyay 2019; Das 2020). The flood vulnerability factor includes the spatial pattern of population density, household density, and land-use types that collectively influence flood susceptibility; furthermore, it includes infrastructure features and educational capacity like flood shelter zones, distance to major roads, distance to hospital, and literacy that in combine act as resilience capacity to cope with flood risk (Table 7).

### Population density

Some natural phenomenon generally triggers natural hazards, and these threats transform into a tragedy when individuals, cultures, and facilities are adversely impacted. As a result, human beings are at the center of disaster and vulnerability. According to many researchers, regions having higher population density have a greater risk of casualties and collateral loss (Kandilioti and Makropoulos 2012; Ngo et al. 2018; Das 2020). Flood risk vulnerability is expected to be higher in areas with poor living conditions, such as overcrowding, malnourishment, and limited access to health care services. However, the population density of the Jalpaiguri district is categorized into four classes (Fig. 4a).



**Table 7** Sub-criteria of selected vulnerability parameters with their assigned and normalized ranks

Parameters	Normalized AHP weights	Sub-classes	Rank	Normalized rank
Population density	0.20	<322	1	0.10
		322–575	2	0.20
		575–646	3	0.30
		>646	4	0.40
Household density	0.18	<70	1	0.1
		70–134	2	0.2
		134–148	3	0.3
		>148	4	0.4
Land use	0.16	Settlement	5	0.28
		Water bodies	5	0.28
		Agriculture land	3	0.17
		Sand bank	2	0.11
		Tea garden	2	0.11
		Vegetation	1	0.06
		Distance from major roads	0.13	0–500
500–1000	2	0.13		
1000–1500	3	0.20		
1500–2000	4	0.27		
Outside buffer	5	0.33		
Distance to flood shelter	0.13	0–1000	1	0.10
		1000–2000	2	0.20
		2000–3000	3	0.30
		Outside buffer	4	0.40
Distance to hospital	0.11	0–1000	1	0.10
		1000–2000	2	0.20
		2000–3000	3	0.30
		Outside buffer	4	0.40
Literacy rate	0.09	<61.50	4	0.40
		61.50–67.00	3	0.30
		67.00–72.02	2	0.20
		>72.02	1	0.10

### Household density

In addition to population density, household density is another factor that directly affects flood vulnerability in low-lying areas due to the potential increase in the exposure of buildings (Tapsell et al. 2002; Cardona 2005). Household density is closely associated with flood risk because it has the potential to influence the severity of flood vulnerability (Ghosh and Kar 2018). In this study, the household density of the Jalpaiguri district can be categorized into four classes (Fig. 4b), and the higher the household density, the higher the chance of casualty and property damage.

### Landuse

The land use pattern of a region demonstrates the utilization of topography by living humans and the natural factors (Ajin

et al. 2013; Kaur et al. 2017). Various hydrological processes, such as surface runoff, infiltration rate, and evapotranspiration in a region, are substantially controlled by the pattern of land use (Yalcin et al. 2011; Darabi et al. 2018). Anthropological practices, such as deforestation and urbanization, directly affect environmental disasters, and the areas with huge settlements are more vulnerable to flooding; hence, land use is a significant parameter in flood vulnerability mapping (Komolafe et al. 2018). However, the area of research can be divided into six land use practice groups (Fig. 4c), and the Kappa accuracy of the land use and land cover map is 91%.

### Distance to roads

Highways inundated during significant rains, contributing to severe connectivity and accessibility difficulties (Das 2020).

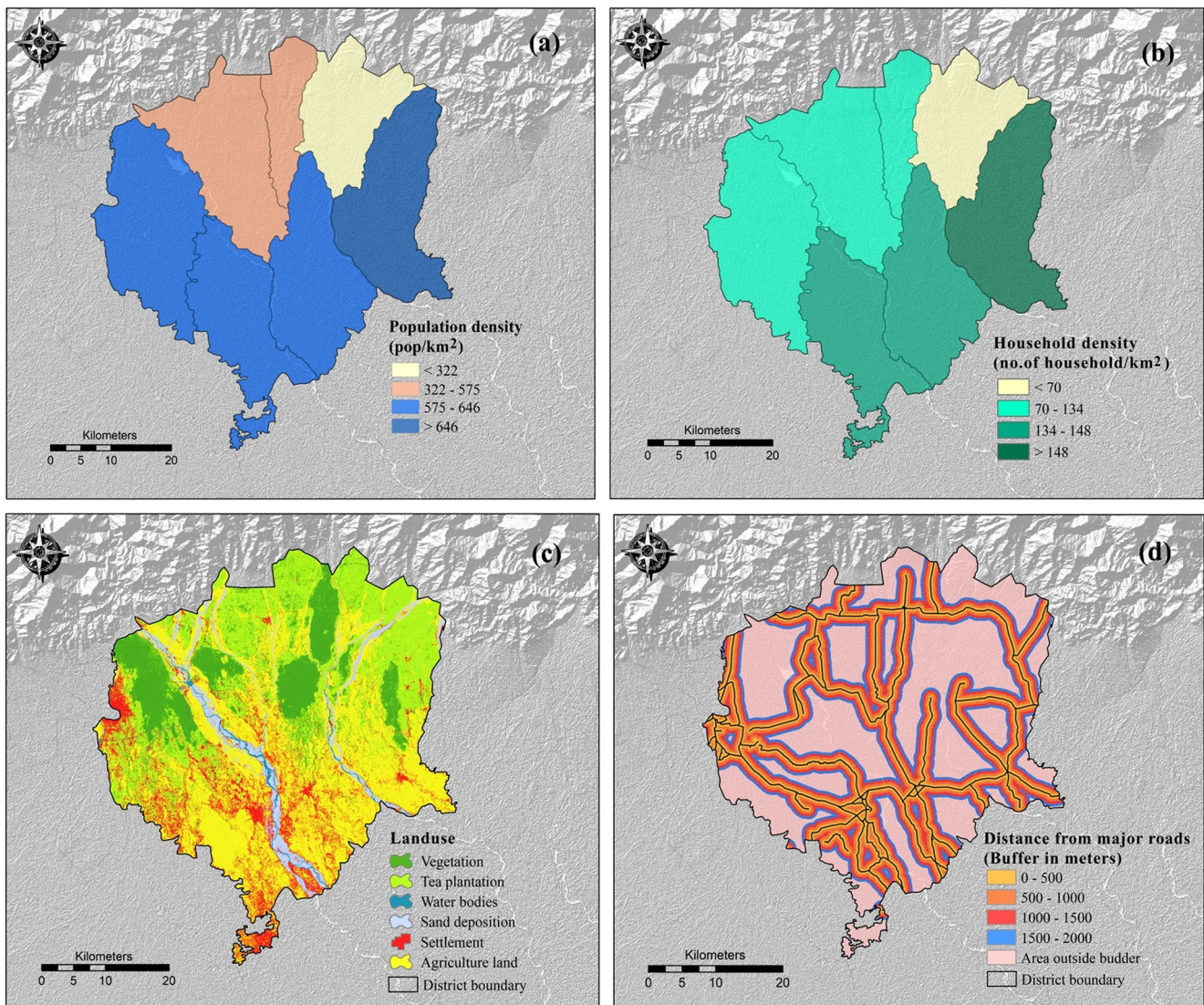


**Fig. 4** Flood vulnerability factors (a) population density, (b) household density, (c) landuse, (d) distance to major roads, (e) distance to flood rescue shelter, (f) distance to hospital, (g) literacy rate

Besides, during flood incidence, the availability of major roads plays a vital role, especially with regard to the provision of relief work, because all rescue and assistance are only possible through major national and state highways (Ghosh and Kar 2018). Thus, in this study, distance to the road is considered as a vulnerability indicator where more the distance from the road indicates more risk to flood (Fig. 4d).

### Distance to flood shelter

During flood incidents, residents are forced to evacuate their houses owing to the risk of casualty. As a result, displaced people are more fragile and vulnerable during the inundation because their protection, safety, health, and sanitation are compromised. Therefore, those away from the proximity to flood rescue zones are at more risk (Hazarika et al. 2018;

Ghosh and Kar 2018). Hence in this study, distance to flood shelters are categorized into four classes (Fig. 4e), and as the distance from the flood shelters increases, vulnerability and risk to flood hazard also increase significantly.

### Distance to hospital

Access to medical service is very much crucial after flood hazard. Effective hazard response needs an adequate number of hospital beds and medically trained as well as technical personnel once there are casualties (Chen et al. 2013). For this reason, in this study, the medical institutions, both governmental and privately owned are taken into consideration for flood vulnerability analysis. Here the distances from hospitals are represented as more the distance from medical service means more flood vulnerability (Fig. 4f)



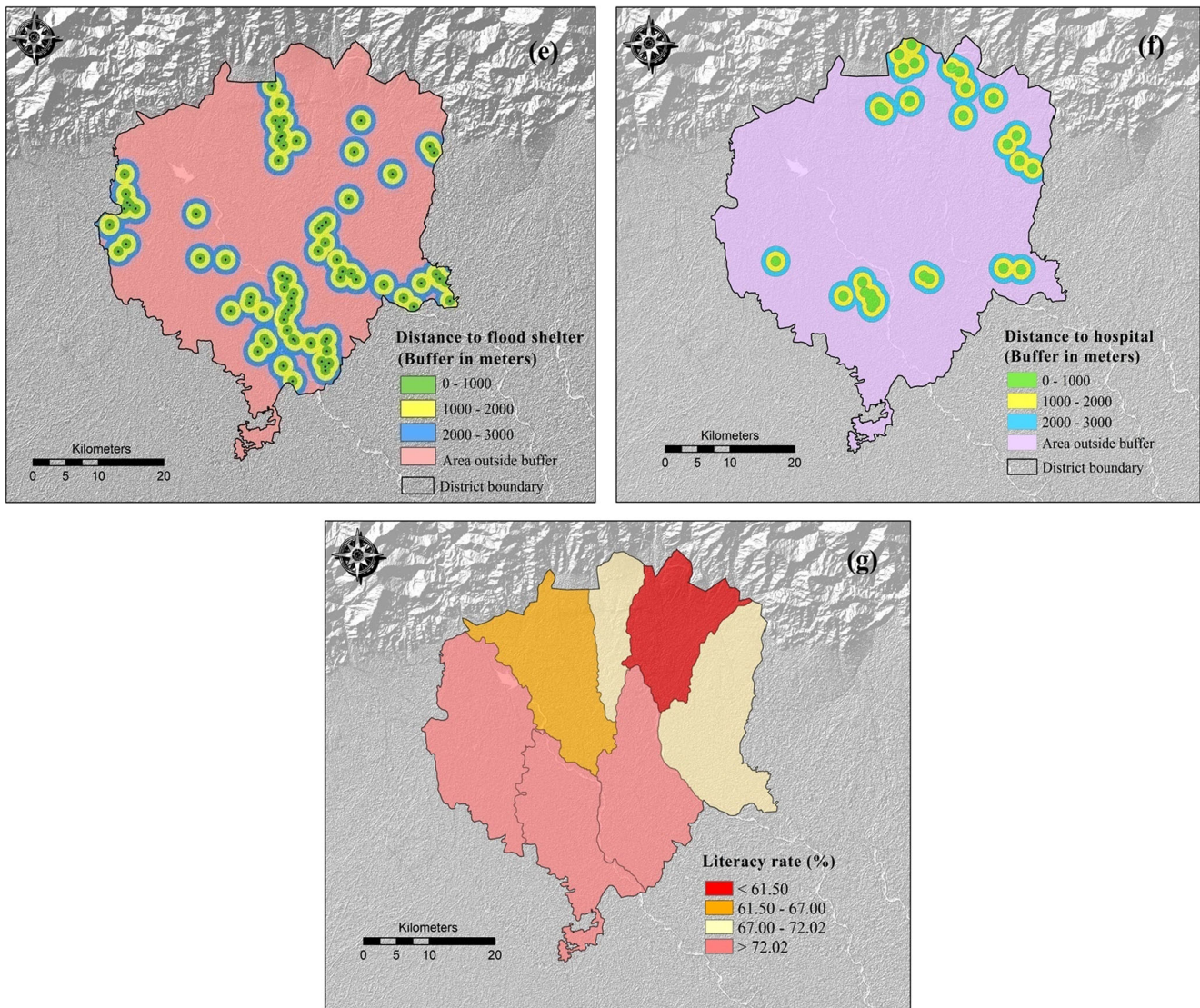


Fig. 4 continued.

## Literacy

The literacy rate is proportional to the literate population of an area's total population. Literacy rates are typically highly critical in recognizing environmental disasters, their severity, and their responses. Consequently, areas with a high literate population are less vulnerable to environmental hazards (Das 2020; Ghosh and Kar 2018). However, literacy rates in the sub-Himalayan Jalpaiguri can be classified into five groups (Fig. 4g).

## RESULT AND DISCUSSION

### Spatial distribution of flood susceptibility

In this present study, ten parameters are used to delineate the flood susceptibility map. However, many researchers used a

variety of parameters to prepare a flood susceptibility map based on the availability and convenience of data. Few studies show that only four parameters are used to demarcate the susceptibility map (Elkhrachy 2015; Kazakis et al. 2015), while some used ten or more than ten geo-environmental indicators (Haghizadeh et al. 2017; Zhao et al. 2018; Ngo et al. 2018; Khosravi et al. 2019; Mirzaei et al. 2020). Furthermore, the accuracy of the susceptibility mapping does not just depend on the criteria selected rather than the quality of spatial datasets, accurate conventional information, field investigation, and expert-based opinion for ranking is the most crucial factor (Ghosh and Kar 2018; Das 2019).

The final outcome of the map can be classified into five classes very low (1.1 km<sup>2</sup>: 0.03%), low (280 km<sup>2</sup>: 8.27%), moderate (1806.5 km<sup>2</sup>: 53.36%), high (1281.4 km<sup>2</sup>: 37.85%), and very high (16.7 km<sup>2</sup>: 0.49%) (Fig. 5 and Table 8). A



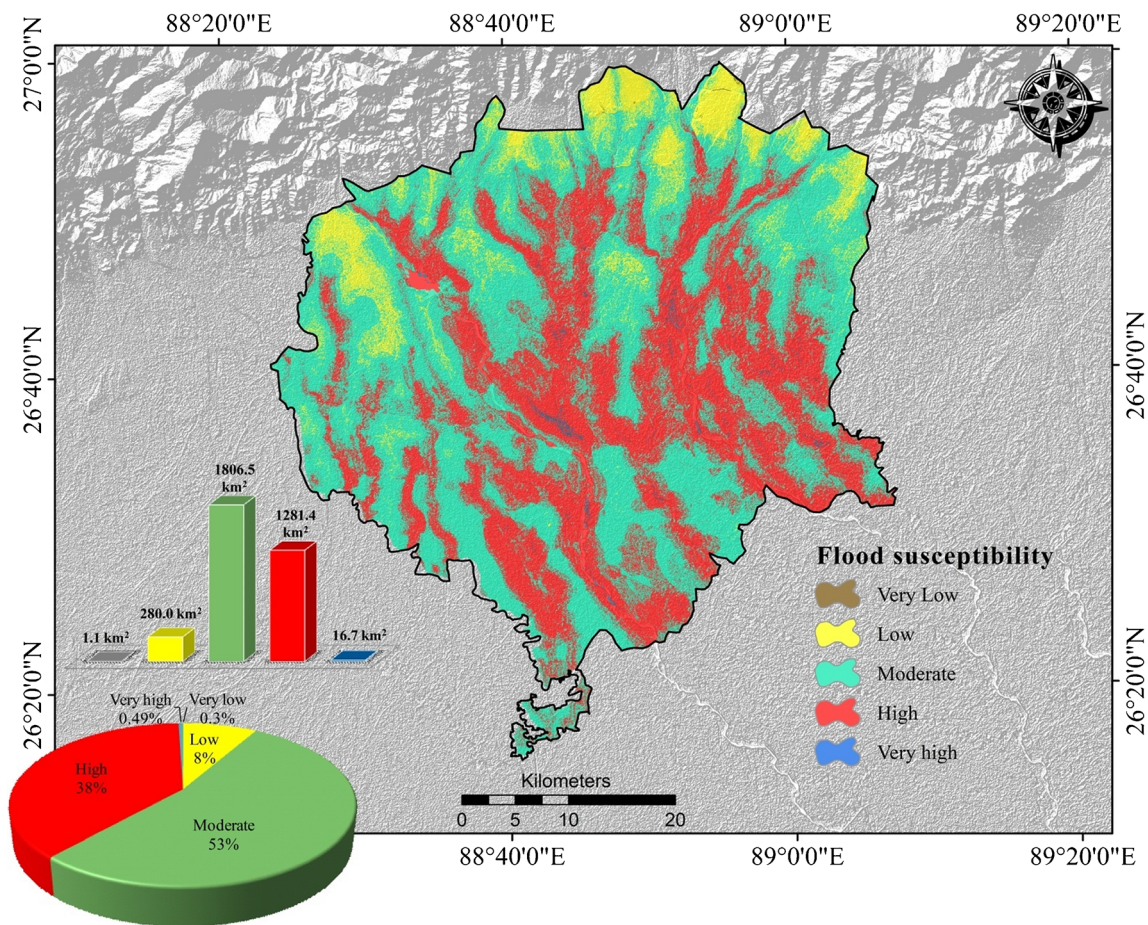


**Fig. 5** Flood susceptibility map of the Jalpaiguri foothill region based on analytical hierarchy process (AHP). The inserted bar diagram representing area distribution (sq.km) and pie diagram indicating percentage of area under flood susceptibility zone

Careful observation according to the map reveals that most of the “high” and “very high” flood-prone areas are situated in the inter-fluvial domain of the southern part along with the flood plain areas and river basins. Furthermore, it is apparent that highly susceptible flood-prone areas are located in areas with a combination of low altitude, less slope, higher drainage density, high TWI, proximity to the rivers, and other variables that induces flood.

**Spatial distribution of flood vulnerability**

The vulnerability index of the study area is prepared based on the seven parameters for the final map preparation, based on the derived normalized AHP weights using the GIS environment. The vulnerability map can be classified into four classes viz. low (97.22km<sup>2</sup>: 2.9%), moderate (1315.90 km<sup>2</sup>: 38.9%), high (1768.77 km<sup>2</sup>: 52.2%), and very high (203.71 km<sup>2</sup>: 6%).

**Table 8** Area and percentage distribution flood susceptibility, vulnerability and risk

Classes	Flood susceptibility			Flood vulnerability			Flood Risk		
	Area (km <sup>2</sup> )	Percentage	Colour indication	Area (km <sup>2</sup> )	Percentage	Colour indication	Area (km <sup>2</sup> )	Percentage	Colour indication
Very low	1.1	0.03		-	-	-	246.0	7.3	
Low	280.0	8.3		97.2	2.9		855.8	25.3	
Moderate	1806.5	53.4		1315.9	38.9		1328.3	39.2	
High	1281.4	37.8		1768.8	52.2		834.0	24.6	
Very high	16.7	0.5		203.7	6.0		121.5	3.6	
Total	3385.6	100.0	-	3385.6	100.0	-	3385.6	100.0	-



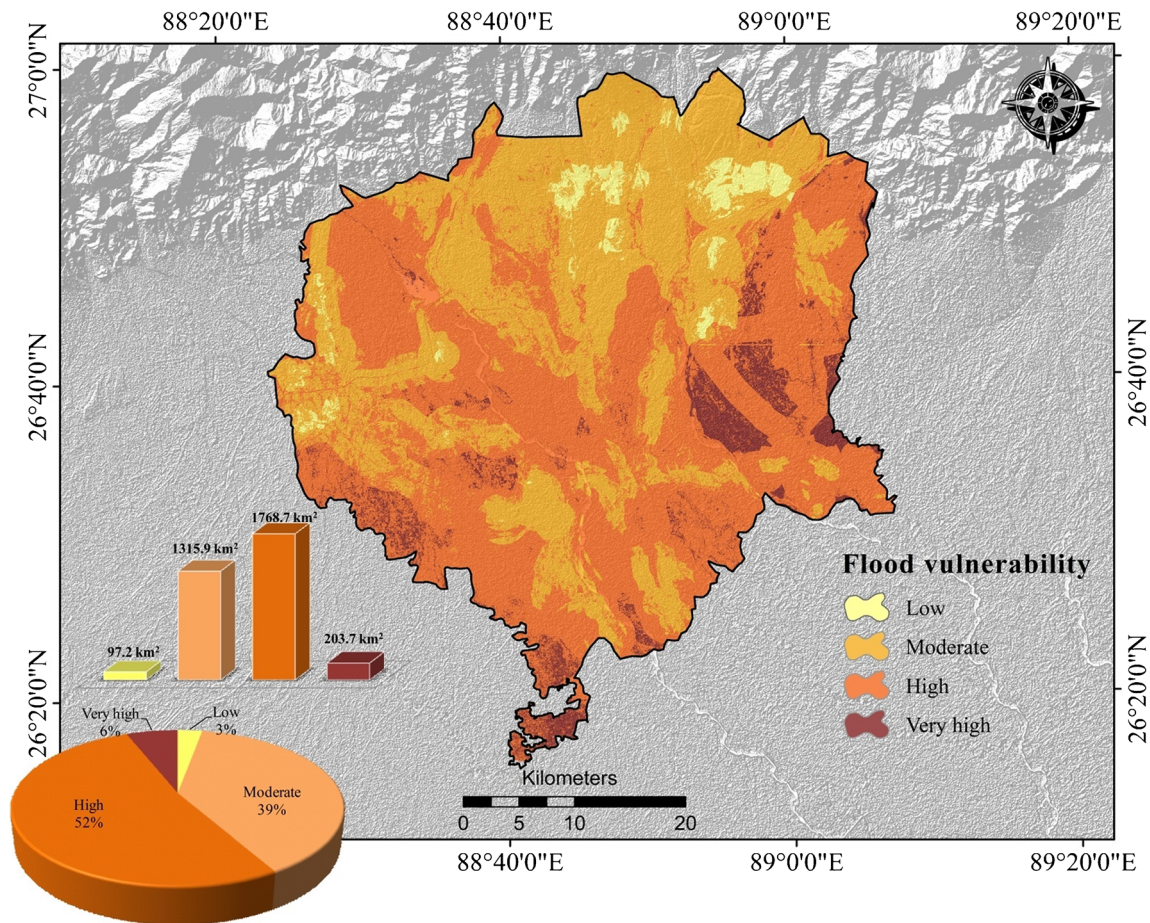


**Fig. 6** Flood vulnerability map of the Jalpaiguri foothill region based on analytical hierarchy process (AHP). The inserted bar diagram representing area distribution (sq.km) and pie diagram indicating percentage of area under flood vulnerability zone

Table 8 and Fig. 6 indicate that most of the Jalpaiguri district covers under “high” vulnerability zone. Furthermore, it reveals that areas with high population and household density, zone of high settlement concentration, and cultivated areas along the river banks have high to very high vulnerable zones, mainly covering the southern and eastern parts. Subsequently, areas near flood rescue shelters, hospitals, and major roads are less vulnerable due to better accessibility. Moreover, a low literacy rate in the entire Jalpaiguri region further ameliorates the vulnerability prospects.

**Flood risk and its distribution**

The sub-Himalayan Jalpaiguri district is endowed with numerous rivers, which became highly erratic, consequences in extensive riverbank erosion, course shifting, and leaving thousands of homeless during the rainy seasons. The majority of the river originates from the same source of the Himalayas, results in frequent floods during periods of heavy rain, and concurrently, all the rivers converge to create a single massive sheet of water, which intensified the flood risk in the entire Jalpaiguri district. Due to heavy rainfall, almost all the study

area’s administrative divisions are affected more or less by the risk of inundation every year. As the entire sub-Himalayan Jalpaiguri is almost flat and covered by alluvial and flood plain except for the northern section, it intensified the risk of stagnation of floodwater for a prolonged period. Subsequently, high population density and continuous expansion of settlements along the river banks resulted in a more vulnerable situation. Furthermore, a few rescue zone, insufficient resilience capacity, and inadequate awareness among people make the situation worse. However, the prepared flood risk map (Fig. 7) indicates that about 28.2% or 955.5km<sup>2</sup> of sub-Himalayan Jalpaiguri falls under high to very high flood risk zone. Table 8 shows that about 7.3%, 25.3%, and 39.2% area falls under the very low, low, and moderate flood risk category, respectively.

Figure 8(a–i) shows the block-wise distribution of flood risk, and it reveals that Dhupguri administrative block has a high risk of flood incidents (212.7km<sup>2</sup>), followed by Maynaguri (187.9 km<sup>2</sup>), Jalpaiguri (174.1 km<sup>2</sup>), Mal (137.3 km<sup>2</sup>), and Rajganj (99.6 km<sup>2</sup>). Besides, the Dhupguri block (Fig. 8g), which is under high threat of inundation, is mainly due to the mighty Jaldhaka river, which flows along the



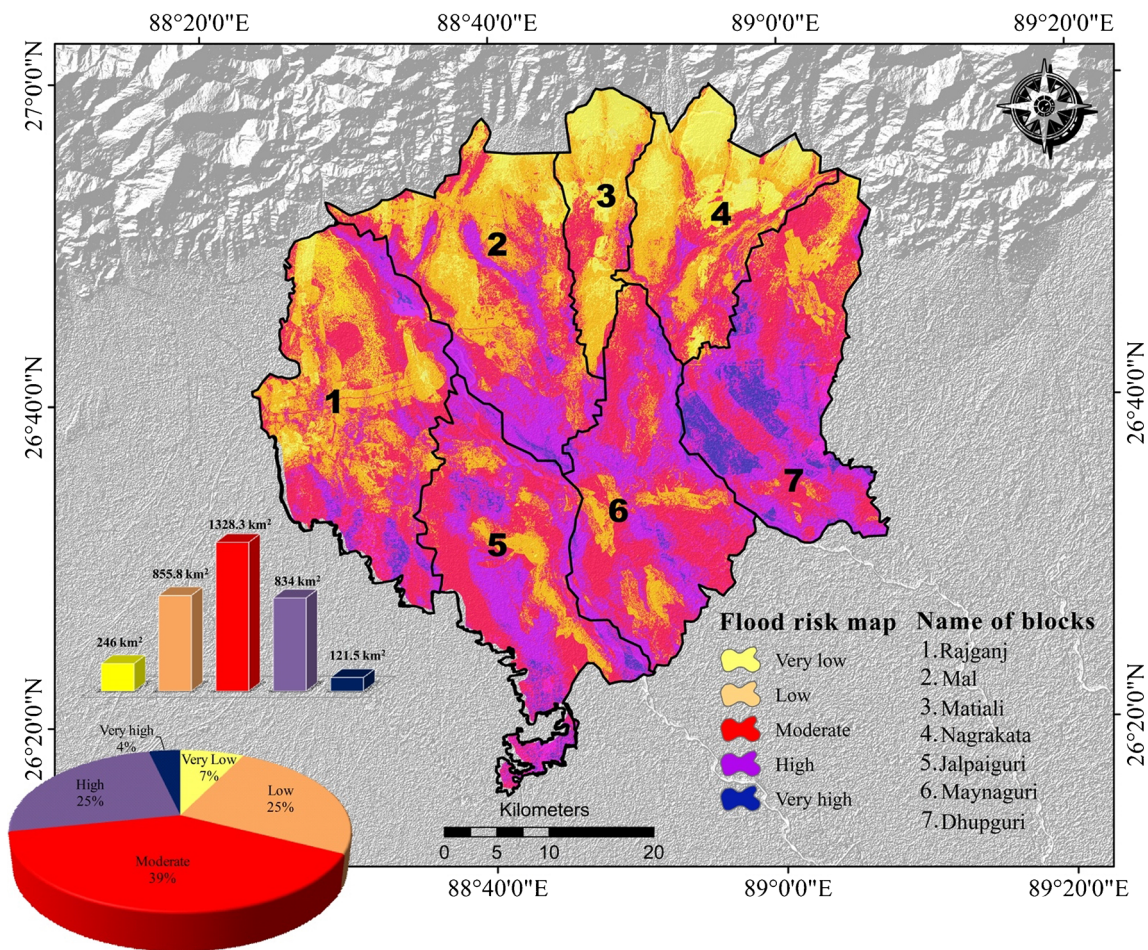


**Fig. 7** Spatial distribution of flood risk zones over the study area. The inserted bar diagram representing area distribution (sq.km) and pie diagram indicating percentage of area under flood risk zone

western margin, is the primary cause that influences flood. However, except for Jaldhaka, there are several other rivers viz. Rethi, Duduya, Kumlai, and others which are responsible for frequent floods in the Dhupguri block of Jalpaiguri sub-Himalaya. On the other hand, the Maynaguri block (Fig. 8f) is affected by the river Teesta and Dharala, Jalpaiguri block by Teesta and Karala (Fig. 8e), Mal and Rajganj block by Teesta and Mahananda, respectively (Fig. 8b and a). Subsequently, Mal, Nagrakata, and Matili blocks have a low risk of flood inundation, mainly due to elevated topography (Fig. 8 b, c, and d). However, instead of its low risk, there is a high chance of flood inundation, mainly along the river banks of these three blocks. So it is clear that the areas situated near the river banks and flood plain region with other vulnerable indicators consequences in high to very high risk of flood, whereas the elevated interfluvial areas of Jalpaiguri have the moderate to very low risk. Furthermore, the entire Jalpaiguri foothill region is undoubtedly more or less vulnerable to flood risk, and hence mitigation strategy and preparedness should be the topmost priority.

### Validation

After developing any model, data validation is one of the most critical tasks to verify the outcome. However, there are numerous methods to validate the MCDM models, but in spatial earth science, the area under the curve (AUC) is the most accurate tools to verify the proficiency of the results due to its simplistic design, comprehensiveness, and fair forecasting nature (Tehrany et al. 2014; Darabi et al. 2018; Malik et al. 2020).

For our present research, the AUC is prepared based on the flood inventory points (field investigation of flood sites, historical records, and literature review). The final AUC curve is computed using the cumulative percentage of area under flood susceptibility and the cumulative percentage of the incidences of flood occurrences (Fig. 9). The accuracy of the AUC curve can be classified into 0.9–1 (excellent), 0.80–0.90 (very good), 0.70–0.80 (good), 0.60–0.70 (poor), 0.50–0.60 (weak) (Rimba et al. 2017; Arabameri et al. 2019). According to the present study, an AUC of 0.862 or 86.2% can be considered excellent for the prepared model. Figure 10 (a–f) shows some major flood events captured during the period of 2017–2019.

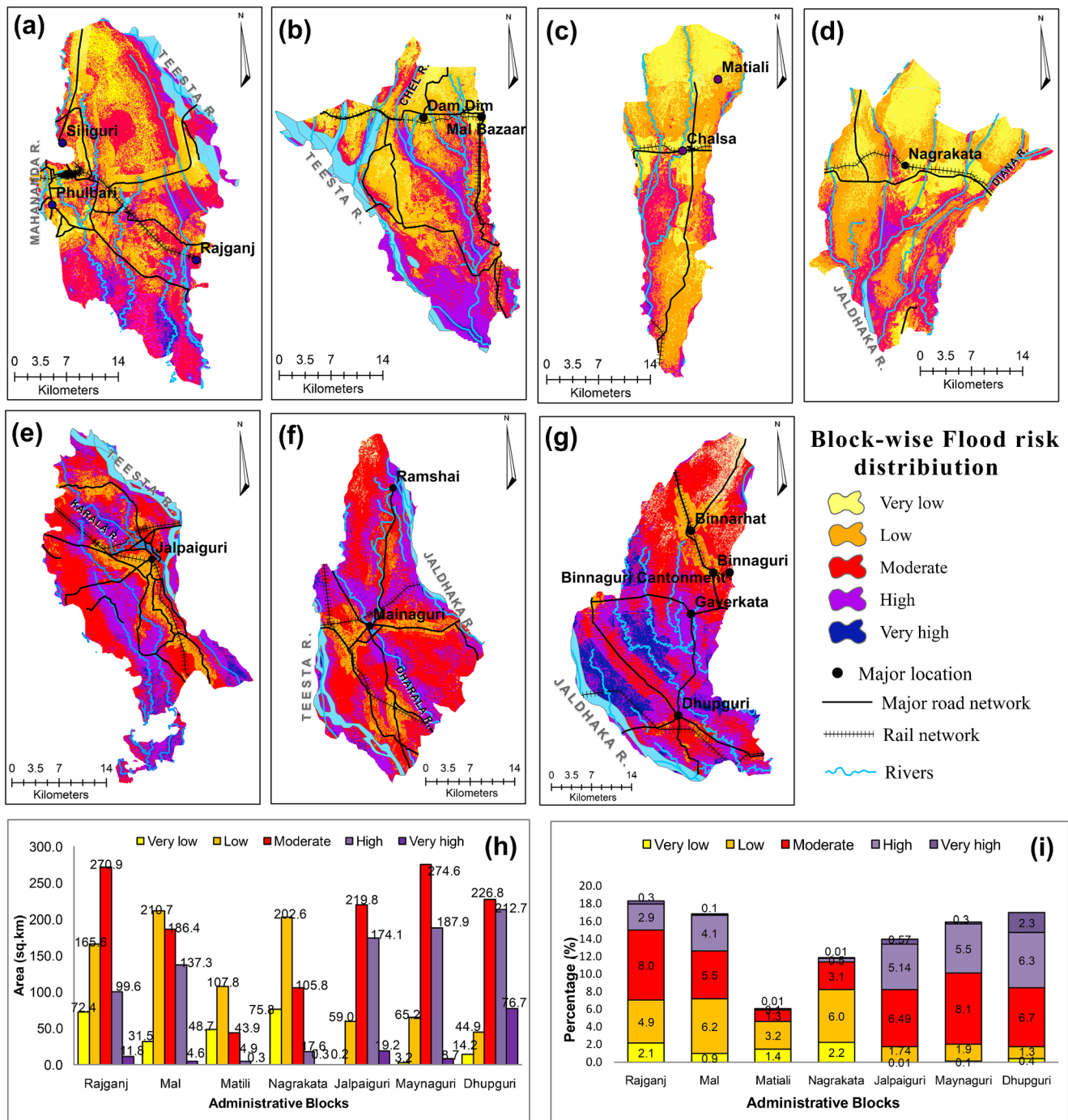


**Fig. 8** Flood risk distribution at administrative level of Jalpaiguri foothill region (a) Rajganj block, (b) Mal block, (c) Matiali block, (d) Nagrakata block, (e) Jalpaiguri block, (f) Maynaguri block, (g) Dhupguri block, (h)

bar diagram representing block-wise area distribution (sq.km) of flood risk., (i) stacked bar diagram indicating block-wise percentage distribution of flood risk

### Conclusion

The present study evaluates the flood risk at the micro-level by considering the parameters including flood susceptibility and vulnerability using a multi-criteria decision method quantitatively based on multiple indicators. Consequently, the three required inputs on flood control, i.e., flood susceptibility,

vulnerability, and risk, have been extensively analyzed and mapped to assess the level of flood danger and track the disaster's footprints. Moreover, this research work rationally combines the geomorphic and hydrological dimensions with the severity of the flood and socio-economic, demographic, and infrastructural elements with the degree of vulnerability. Since both susceptibility and vulnerability are essential factors



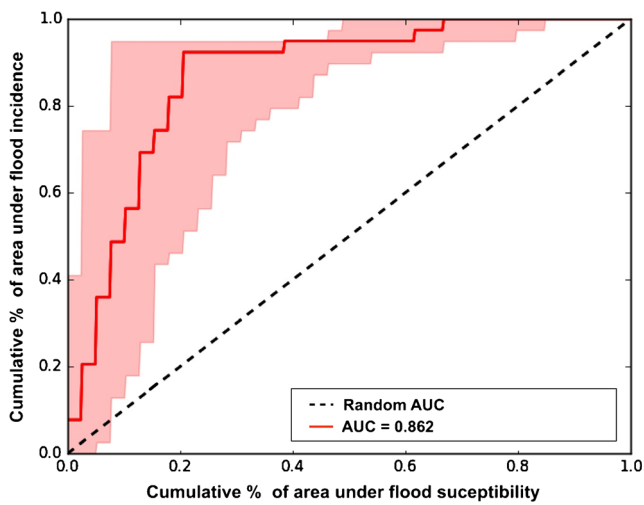


**Fig. 9** Validation of model using area under curve (AUC). The final AUC is 0.862 or 86.2%

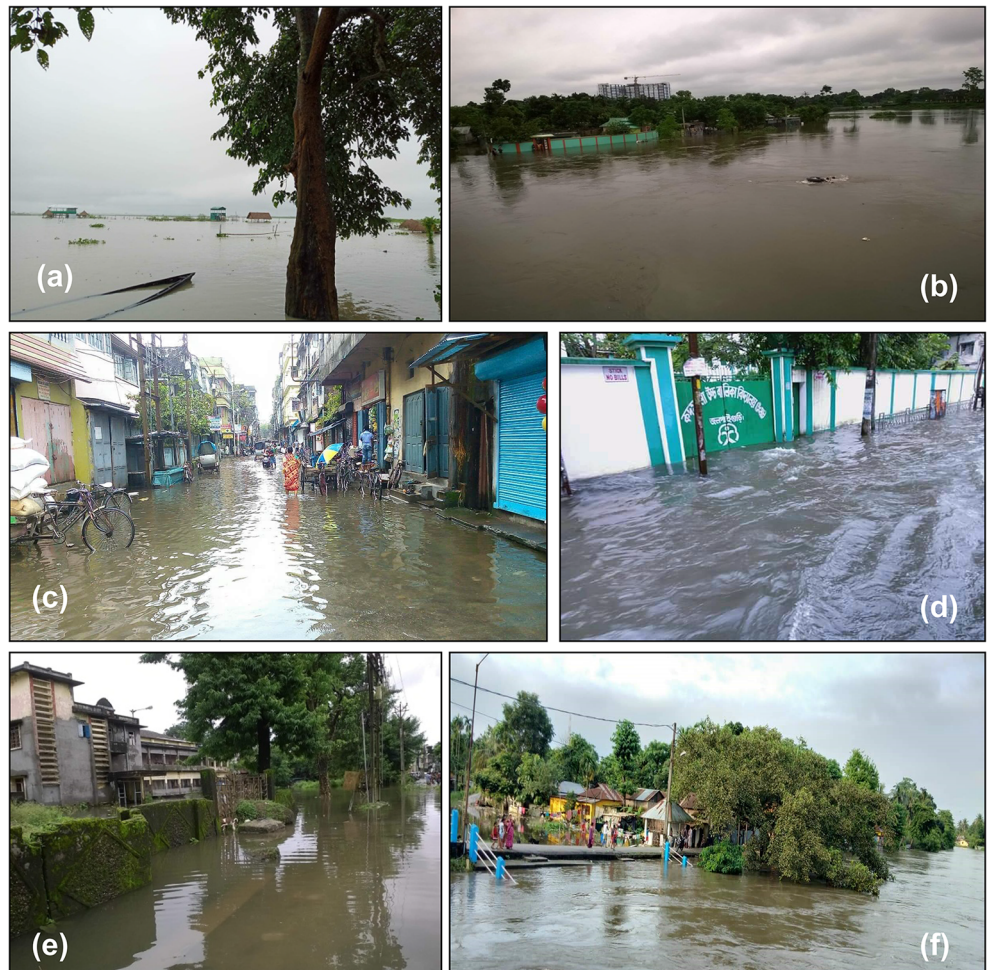
to assess the intensity of risk, that will further define the target areas for successful preparation of safety planning measures. Furthermore, the current study has been thoroughly validated

so that it can be applied with confidence to the target areas in the context of mitigation policies.

The Himalayan foothill region encounters regular floods of high magnitude, resulting in colossal infrastructure damage and extreme socio-economic destruction. Therefore, the devastation due to flood hazards demonstrated the urgent need for risk management to understand flood risk elements in a better way. Moreover, the present research outcome indicates that low-lying flood plain areas and the river basins are more prone to flood risk, which further combines with havoc population, insufficient resilience capacity, and inadequate infrastructure results the situation into mayhem. This study is focused on a wide range of effective parameters reported from different research studies, performed in various corners of the world and can therefore act as first-hand documentation and can be a revolutionary finding for data-lacking Himalayan foothill region, presented before larger scientific platforms.

Subsequently, flood risk assessment at the administrative level is beneficial for the local executive bodies to take imperative strategies and formulate necessary flood control planning. It can be recommended to prioritize understanding the

**Fig. 10** Glimpse of flood affected areas at Jalpaiguri foothill region (a) Teesta spur completely submerged under flood, (b) near Jalpaiguri engineering college, (c) flood at Rajganj, (d) Kadamtala school near DBC road fully inundated due to flood, (e) flood at Dhupguri block, (f) River karala enters Jalpaiguri town near Maskalaibari due to intense rain



floodplain region and its impacts on the local people's livelihood. Further, flood defense systems, including structural mitigation and non-structural mitigation, need to be more highlighted. Also, steps like the prohibition of settlement encroachment, more accessibility to flood shelters and hospitals, proper flood plain usage, flood insurance, and most notably, public consciousness should be of utmost importance to mitigate flood risk of the Himalayan foothill region. The flood susceptibility, vulnerability, and flood risk mapping of the present study can be beneficial for the policymakers, administrative bodies, environmentalists, and engineers for flood prevention and can be applied for the different flood-prone regions around the world.

**Acknowledgements** The author wishes thanks to the Department of Geography and Applied Geography, University of North Bengal, for providing the necessary facilities to conduct this research. Also, the authors would like to acknowledge Mr. Gopal Das, Assistant teacher of Geography, Maynaguri Subhas Nagar High School, for his support during the field investigation, without which it is not possible to find such novel results. Besides, the authors would like to express their sincere gratitude to the Editor-in-chief Abdullah Al-Amri and Prof. Biswajeet Pradhan for their insightful suggestions and comments, which immensely helped in the improvement of the earlier version of the manuscript. Subsequently, the constructive comments from two anonymous reviewers significantly improved the quality of the manuscript. Lastly, the author would like to thank Mr. Nimai Singha and Mr. Debanjan Basak, research scholar of CBPBU and NBU for their support throughout the study.

**Declarations** This research study is carried out in compliance with field knowledge, transparency, moral values and hard work.

**Ethics approval** Not applicable

**Consent to participate** All the co-authors read this article before submission and every step are informed to all the co-authors.

**Conflict of Interest** The authors declare that they have no competing interests.

## References

- Adhikari P, Hong Y, Douglas KR, Kirschbaum DB, Gourley J, Adler R, Brakenridge GR (2010) A digitized global flood inventory (1998–2008): compilation and preliminary results. *Nat Hazards* 55(2):405–422. <https://doi.org/10.1007/s11069-010-9537-2>
- Ali KR, Ahmad A, Ahmad SN (2019) Application of GIS-based analytic hierarchy process and frequency ratio model to flood vulnerable mapping and risk area estimation at Sundarban region, India. *Model Earth Syst Environ* 5:1083–1102. <https://doi.org/10.1007/s40808-019-00593-z>
- Arabameri A, Rezaei K, Cerda A, Conoscenti C, Kalantari Z (2019) A comparison of statistical methods and multi-criteria decision making to map flood hazard susceptibility in Northern Iran. *Sci Total Environ* 660:443–458. <https://doi.org/10.1016/j.scitotenv.2019.01.021>
- Arefin R (2020) Groundwater potential zone identification at Plio-Pleistocene elevated tract, Bangladesh: AHP-GIS and remote sensing approach. *Groundw Sustain Dev* 10:100340. <https://doi.org/10.1016/j.gsd.2020.100340>
- Arya AK, Singh AP (2021) Multi criteria analysis for flood hazard mapping using GIS techniques: a case study of Ghaghara River basin in Uttar Pradesh, India. *Arab J Geosci* 14:656. <https://doi.org/10.1007/s12517-021-06971-1>
- Ajin RS, Krishnamurthy RR, Jayaprakash M, Vinod PG (2013) Flood hazard assessment of Vamanapuram River basin, Kerala, India: an approach using remote sensing & GIS techniques. *Adv Appl Sci Res* 4(3):263–274
- Benjmel K, Amraoui F, Boutaleb S (2020) Mapping of Groundwater Potential Zones in Crystalline Terrain Using Remote Sensing, GIS Techniques, and Multicriteria Data Analysis (Case of the Ighrem Region, Western Anti-Atlas, Morocco). *Water*. <https://doi.org/10.3390/w12020471>
- Balica SF, Wrightm NG, Meulen FV (2012) A flood vulnerability index for coastal cities and its use in assessing climate change impacts. *Nat Hazards* 64:73–105. <https://doi.org/10.1007/s11069-012-0234-1>
- Bui DT, Panahi M, Shahabi H, Singh VP, Shirzadi A, Chapi K, Khosravi K, Chen W, Panahi S, Li S, Bin AB (2018) Novel Hybrid Evolutionary Algorithms for Spatial Prediction of Floods. *Sci Rep* 8:15364. <https://doi.org/10.1038/s41598-018-33755-7>
- Bui DT, Pradhan B, Nampak H, Bui QT, Tran QA, Nguyen QP (2016) Hybrid artificial intelligence approach based on neural fuzzy inference model and metaheuristic optimization for flood susceptibility modeling in a high-frequency tropical cyclone area using GIS. *J Hydrol* 540:317–330. <https://doi.org/10.1016/j.jhydrol.2016.06.027>
- Bui DT, Khosravi K, Shahabi H, Daggupati P, Adamowski JF, Melesse AM, Thai Pham B, Pourghasemi HR, Mahmoudi M, Bahrami S, Pradhan B, Shirzadi A, Chapi K, Lee S (2019) Flood Spatial Modeling in Northern Iran Using Remote Sensing and GIS: A Comparison between Evidential Belief Functions and Its Ensemble with a Multivariate Logistic Regression Model. *Remote Sens* 11(13):1589. <https://doi.org/10.3390/rs11131589>
- Cardona O (2005) Indicators of disaster risk and risk management: Summary report. Inter-American Development Bank. [https://www.ipcc.ch/apps/nj-lite/srex/nj-lite\\_download.php?id=6132](https://www.ipcc.ch/apps/nj-lite/srex/nj-lite_download.php?id=6132)
- Census of India (2011) District Census Handbook, Jalpaiguri. Retrieved from [https://censusindia.gov.in/2011census/dchb/DCHB\\_A/19/1902\\_PART\\_A\\_DCHB\\_JALPAIGURI.pdf](https://censusindia.gov.in/2011census/dchb/DCHB_A/19/1902_PART_A_DCHB_JALPAIGURI.pdf)
- Chakraborty S, Datta K (2013) Causes and Consequences of Channel Changes – A Spatio-Temporal Analysis using Remote Sensing and Gis— Jaldhaka-Diana River System (Lower Course), Jalpaiguri (Duars), West Bengal, India. *J Geogr Nat Disast* 3:107. <https://doi.org/10.4172/2167-0587.1000107>
- Chakraborty S (2017) Dynamics of hydro-geomorphological environment in Jaldhaka river basin of West Bengal and its impacts on landuse. Unpublished Ph.D. thesis, Visva-Bharati, Santiniketan. <http://hdl.handle.net/10603/227699>
- Chakraborty S, Mukhopadhyay S (2019) Assessing flood risk using analytical hierarchy process (AHP) and geographical information system (GIS): application in Coochbehar district of West Bengal, India. *Nat Hazards* 99(1):247–274. <https://doi.org/10.1007/s11069-019-03737-7>
- Chen W, Cutter SL, Emrich CT, Shi P (2013) Measuring social vulnerability to natural hazards in the Yangtze River Delta region, China. *Int J Disaster Risk Sci* 4(4):169–181. <https://doi.org/10.1007/s13753-013-0018-6>
- Chen W, Li Y, Xue W, Shahabi H, Shaojun LH, Hong X, Wang H, Bian S, Zhang B, Pradhan B, Ahmad (2019) Modeling flood susceptibility using data-driven approaches of naïve Bayes tree, alternating decision tree, and random forest methods. *Sci Total Environ* 701:134979. <https://doi.org/10.1016/j.scitotenv.2019.134979>



- Danumah JH, Odai SN, Saley BM, Szarzynski J, Thiel M, Kwaku A, Kouame FK, Akpa LY (2016) Flood risk assessment and mapping in Abidjan district using multi-criteria analysis (AHP) model and geoinformation techniques, (coted'ivoire). *Geoenviron Disasters* 3: 10. <https://doi.org/10.1186/s40677-016-0044-y>
- Dano UL, Balogun AL, Matori AN, Wan Yusouf K, Abubakar IR, Said Mohamed MA, Aina YA, Pradhan B (2019) Flood susceptibility mapping using GIS-based analytic network process: A case study of Perlis, Malaysia. *Water* 11(3):615. <https://doi.org/10.3390/w11030615>
- Darabi H, Choubin B, Rahmati O, Haghghi AT, Pradhan B, Kløve B (2018) Urban flood risk mapping using the GARP and QUEST models: A comparative study of machine learning techniques. *J Hydrol* 569:142–154. <https://doi.org/10.1016/j.jhydrol.2018.12.002>
- Das M, Chattopadhyay A, Basu R (2017) Spatial Flood Potential Mapping (SFPMP) with Flood Probability and Exposure Indicators of Flood Vulnerability: Case Study Former Jalpaiguri District, West Bengal, India. *J Geogr Nat Disast* 7:210. <https://doi.org/10.4172/2167-0587.1000210>
- Das S (2018) Geographic information system and AHP-based flood hazard zonation of Vaitama basin, Maharashtra, India. *Arab J Geosci* 11:576. <https://doi.org/10.1007/s12517-018-3933-4>
- Das S (2019) Geospatial mapping of flood susceptibility and hydrogeomorphic response to the floods in Ulhas basin, India. *Remote Sens Appl: Society and Environment* 14:60–74. <https://doi.org/10.1016/j.rsase.2019.02.006>
- Das S (2020) Flood susceptibility mapping of the Western Ghat coastal belt using multi-source geospatial data and analytical hierarchy process (AHP). *Remote Sensing Appl: Society and Environment* 20: 100379. <https://doi.org/10.1016/j.rsase.2020.100379>
- de Brito MM, Evers M (2016) Multi-criteria decision-making for flood risk management: a survey of the current state of the art. *Nat Hazards Earth Syst Sci* 16(4):1019–1033. <https://doi.org/10.5194/nhess-16-1019-2016>
- Dhar ON, Nandargi S (2003) Hydrometeorological aspects of floods in India. *Nat Hazards* 28(1):1–33. <https://doi.org/10.1023/A:1021199714487>
- District Census Handbook, Jalpaiguri (2011) Census of India 2011. WEST BENGAL. Retrieved from: [https://censusindia.gov.in/2011census/dchb/DCHB\\_A/19/1902\\_PART\\_A\\_DCHB\\_JALPAIGURI.pdf](https://censusindia.gov.in/2011census/dchb/DCHB_A/19/1902_PART_A_DCHB_JALPAIGURI.pdf)
- El-Haddad BA, Youssef AM, Pourghasemi HR, Pradhan B, El-Shater AH, El-Khashab MH (2020) Flood susceptibility prediction using four machine learning techniques and comparison of their performance at WadiQena Basin, Egypt. *Nat Hazards* 105(1):83–114. <https://doi.org/10.1007/s11069-020-04296-y>
- El-Magd SAA, Pradhan B, Alamri A (2021) Machine learning algorithm for flash flood prediction mapping in Wadi El-Laqeita and surroundings, Central Eastern Desert, Egypt. *Arab J Geosci* 14:323. <https://doi.org/10.1007/s12517-021-06466-z>
- Elkhrachy I (2015) Flash flood hazard mapping using satellite images and GIS tools: a case study of Najran City, Kingdom of Saudi Arabia (KSA). *Egypt J Remote Sens Space Sci* 18(2):261–278. <https://doi.org/10.1016/j.ejrs.2015.06.007>
- Ghosh A (2016) Quantitative approach on erosion hazard, vulnerability and risk assessment: case study of Muriganga–Saptamukhi interfluvium. *Nat Hazards* 87:1709–1729. <https://doi.org/10.1007/s11069-017-2844-0>
- Ghosh A, Kar SK (2018) Application of analytical hierarchy process (AHP) for flood risk assessment: a case study in Malda district of West Bengal, India. *Nat Hazards* 94(1):349–368. <https://doi.org/10.1007/s11069-018-3392-y>
- Ghosh A, Mandal M, Banerjee M, Karmakar M (2020) Impact of hydrogeological environment on availability of groundwater using analytical hierarchy process (AHP) and geospatial techniques: A study from the upper Kangsabati river basin. *Groundw Sustain Dev* 11: 100419. <https://doi.org/10.1016/j.gsd.2020.100419>
- Ghosh M, Ghosal S (2020) Climate change vulnerability of rural households in flood-prone areas of Himalayan foothills, West Bengal, India. *Environ Dev Sustain* 23:2570–2595. <https://doi.org/10.1007/s10668-020-00687-0>
- Gupta S, Javed A, Datt D (2003) Economics of flood protection in India. In: *In Flood Problem and Management in South Asia*. Springer, Dordrecht, pp 199–210. [https://doi.org/10.1007/978-94-017-0137-2\\_10](https://doi.org/10.1007/978-94-017-0137-2_10)
- Haghizadeh A, Siahkamari S, Haghiabi AH, Rahmati O (2017) Forecasting flood-prone areas using Shannon's entropy model. *J Earth Syst Sci* 126(3):39
- Hammami S, Zouhri L, Soueï D, Soueï A, Zghibi Z, Marzougui A, Dlala M (2019) Application of the GIS based multi-criteria decision analysis and analytical hierarchy process (AHP) in the flood susceptibility mapping (Tunisia). *Arab J Geosci* 12:653. <https://doi.org/10.1007/s12517-019-4754-9>
- Handfield R, Walton SV, Sroufe R, Melnyk SA (2002) Applying environmental criteria to supplier assessment: a study in the application of the analytical hierarchy process. *Eur J Oper Res* 141:70–87. [https://doi.org/10.1016/S0377-2217\(01\)00261-2](https://doi.org/10.1016/S0377-2217(01)00261-2)
- Hazarika N, Barman D, Das AK, Sarma AK, Borah SB (2018) Assessing and mapping flood hazard, vulnerability and risk in the Upper Brahmaputra River valley using stakeholders' knowledge and multicriteria evaluation (MCE). *J Flood Risk Manag* 11(52):S700–S716. <https://doi.org/10.1111/jfr3.12237>
- Hindustan times (2016) Bengal floods: 58,000 people affected, red alert issued in Jalpaiguri. Retrieved from: <https://www.hindustantimes.com/india-news/bengal-floods-58-000-people-affected-red-alert-issued-in-jalpaiguri/story-V9c7a9NRZa1kNiuAJc5kO.html>
- Hong H, Pradhan B, Xu C, Bui DT (2015) Spatial prediction of landslide hazard at the Yihuang area (China) using two-class kernel logistic regression, alternating decision tree and support vector machines. *Catena* 133:266–281. <https://doi.org/10.1016/j.catena.2015.05.019>
- Horton RE (1945) Erosional development of streams and their drainage basins: hydrophysical approach to quantitative morphology. *Geol Soc Am Bull* 56(3):275–370. [https://doi.org/10.1130/0016-7606\(1945\)56\[275:EDOSAT\]2.0.CO;2](https://doi.org/10.1130/0016-7606(1945)56[275:EDOSAT]2.0.CO;2)
- Hoque MAA, Tasfia S, Ahmed N, Pradhan B (2019) Assessing spatial flood vulnerability at KalaparaUpazila in Bangladesh using an analytical hierarchy process. *Sensors* 19(6):1302. <https://doi.org/10.3390/s19061302>
- Hu S, Cheng X, Zhou D, Zhang H (2017) GIS-based flood risk assessment in suburban areas: a case study of the Fangshan District, Beijing. *Nat Hazards* 87:1525–1543. <https://doi.org/10.1007/s11069-017-2828-0>
- Ibrahim-Bathis K, Ahmed SA (2016) Geospatial technology for delineating groundwater potential zones in Doddahalla watershed of Chitradurga district. *India Egypt J Remote Sens Space Sci* 19(2): 223–234. <https://doi.org/10.1016/j.ejrs.2016.06.002>
- Kale VS (2004) Floods in India: their frequency and pattern. Coping with natural hazards: Indian context. Orient Longman, Hyderabad, pp 91–103
- Kandilioti G, Makropoulos C (2012) Preliminary flood risk assessment: the case of Athens. *Nat Hazards* 61:441–468. <https://doi.org/10.1007/s11069-011-9930-5>
- Kaur H, Gupta S, Parkash S, Thapa R, Mandal R (2017) Geospatial modelling of flood susceptibility pattern in a subtropical area of West Bengal, India. *Environ Earth Sci* 76(9):339
- Kazakis N, Kougias I, Patsialis T (2015) Assessment of flood hazard areas at a regional scale using an index-based approach and Analytical Hierarchy Process: Application in Rhodope–Evros region, Greece. *Sci of Total Environ* 538:555–563. <https://doi.org/10.1016/j.scitotenv.2015.08.055>

- Khosravi K, Panahi M, Tien Bui D (2018) Spatial prediction of groundwater spring potential mapping based on adaptive neuro-fuzzy inference system and metaheuristic optimization. *Hydrol Earth Syst Sci* 22:4771–4792. <https://doi.org/10.5194/hess-22-4771-2018>
- Khosravi K, Shahabi H, Pham BT, Adamowski J, Shirzadi A, Pradhan B, Dou J, Ly HB, Gróf G, Ho HL, Hong H, Chapi K, Prakash I (2019) A comparative assessment of flood susceptibility modeling using multi-criteria decision-making analysis and machine learning methods. *J Hydrol* 573:311–323. <https://doi.org/10.1016/j.jhydrol.2019.03.073>
- Kittipongvises S, Phetrak A, Rattanapun P, Brundiers K, Buizer JL, Melnick R (2020) AHP-GIS analysis for flood hazard assessment of the communities nearby the world heritage site on Ayutthaya Island, Thailand. *Int J Disaster Risk Reduct* 48:101612. <https://doi.org/10.1016/j.ijdrr.2020.101612>
- Komolafe AA, Herath S, Avtar R (2018) Methodology to assess potential flood damages in urban areas under the influence of climate change. *Nat Hazards Review* 19(2):05018001. [https://doi.org/10.1061/\(ASCE\)NH.1527-6996.0000278](https://doi.org/10.1061/(ASCE)NH.1527-6996.0000278)
- Kim S, Lee W, Shin K, Kafatos M, Seo D, Kwak H (2011) Comparison of spatial interpolation techniques for predicting climate factors in Korea. *For Sci Technol* 6:97–109. <https://doi.org/10.1080/21580103.2010.9671977>
- Kourgialas NN, Karatzas GP (2011) Flood management and a GIS modelling method to assess flood-hazard areas—a case study. *Hydrol Sci J—J des Sci Hydrol* 56(2):212–225. <https://doi.org/10.1080/02626667.2011.555836>
- Kron W, Steuer M, Löw P, Wirtz A (2012) How to deal properly with a natural catastrophe database—analysis of flood losses. *Nat Hazards Earth Syst Sci* 12(3):535–550. <https://doi.org/10.5194/nhess-12-535-2012>
- Ly S, Charles C, Degré A (2013) Different methods for spatial interpolation of rainfall data for operational hydrology and hydrological modeling at watershed scale. A review. *Biotechnol Agron Soc Environ* 17(2):392–406
- Mahalanobis PC (1927) Rainfall and floods in North Bengal. Bengal Secretariat Press, Kolkata, pp 1870–1922
- Malik S, Chandra Pal S, Chowdhuri I, Chakraborty R, Roy P, Das B (2020) Prediction of Highly Flood Prone Areas by GIS Based Heuristic and Statistical Model in a Monsoon Dominated Region of Bengal Basin. *Remote Sens Appl Soc Environ* 19:100343. <https://doi.org/10.1016/j.rsase.2020.100343>
- Mandal S, Sarkar S (2016) Overprint of neotectonism along the course of River Chel, North Bengal, India. *J Palaeogeogr* 5(3):221–240. <https://doi.org/10.1016/j.jop.2016.05.004>
- Merlotto A, Bertola GR, Piccolo MC (2016) Hazard, vulnerability and coastal erosion risk assessment in Necochea Municipality, Buenos Aires Province, Argentina. *J Coast Conserv* 20:351–362. <https://doi.org/10.1007/s11852-016-0447-7>
- Mirzaei S, Vafakhah M, Pradhan B, Alavi SJ (2020) Flood susceptibility assessment using extreme gradient boosting (EGB), Iran. *Earth Sci Inf* 14(1):51–67. <https://doi.org/10.1007/s12145-020-00530-0>
- Mishra K, Sinha R (2020) Flood risk assessment in the Kosimegafan using multi-criteria decision analysis: A hydro-geomorphic approach. *Geomorphology* 350:106861. <https://doi.org/10.1016/j.geomorph.2019.106861>
- Moore ID, Grayson RB, Ladson AR (1991) Digital terrain modelling: a review of hydrological, geomorphological, and biological applications. *Hydrol Process* 5:3–30. <https://doi.org/10.1002/hyp.3360050103>
- Muralitharan J, Palanivel K (2015) Groundwater targeting using remote sensing, geographical information system and analytical hierarchy process method in hard rock aquifer system, Karur district, Tamil Nadu, India. *Earth Sci Inf* 8(4):827–842. <https://doi.org/10.1007/s12145-015-0213-7>
- Nied M, Schröter K, Lüdtke S, Nguyen VD, Merz B (2017) What are the hydro-meteorological controls on flood characteristics? *J Hydrol* 545:310–326. <https://doi.org/10.1016/j.jhydrol.2016.12.003>
- Ngo PTT, Hoang ND, Pradhan B, Nguyen QK, Tran XT, Nguyen QM, Nguyen VN, Samui P, Bui DT (2018) A novel hybrid swarm optimized multilayer neural network for spatial prediction of flash floods in tropical areas using sentinel-1 SAR imagery and geospatial data. *Sensors* 18(11):3704. <https://doi.org/10.3390/s18113704>
- Ogden FL, Raj Pradhan N, Downer CW, Zahner JA (2011) Relative importance of impervious area, drainage density, width function, and subsurface storm drainage on flood runoff from an urbanized catchment. *Water Resour Res* 47(12). <https://doi.org/10.1029/2011WR010550>
- Pourghasemi HR, Pradhan B, Gokceoglu C, Mohammadi M, Moradi HR (2012) Application of weights-of-evidence and certainty factor models and their comparison in landslide susceptibility mapping at Haraz watershed, Iran. *Arab J Geosci* 6(7):2351–2365. <https://doi.org/10.1007/s12517-012-0532-7>
- Pradhan B (2009) Flood susceptible mapping and risk area delineation using logistic regression, GIS and remote sensing. *J Spatial Hydrol* 9:1–18
- Prokop P, Walanus A (2017) Impact of the Darjeeling–Bhutan Himalayan front on rainfall hazard pattern. *Nat Hazards* 89:387–404. <https://doi.org/10.1007/s11069-017-2970-8>
- Rahmati O, Pourghasemi HR, Zeinivand H (2016) Flood susceptibility mapping using frequency ratio and weights-of-evidence models in the Golastan Province. *Iran Geocarto Int* 31:42–70. <https://doi.org/10.1080/10106049.2015.1041559>
- Reneau SL (2000) Stream incision and terrace development in Frijoles Canyon, Bandelier National Monument, New Mexico, and the influence of lithology and climate. *Geomorphology* 32:171–193. [https://doi.org/10.1016/S0169-555X\(99\)00094-X](https://doi.org/10.1016/S0169-555X(99)00094-X)
- Rimba AB, Setiawati MD, Sambah AB, Miura F (2017) Physical Flood Vulnerability Mapping Applying Geospatial Techniques in Okazaki City, Aichi Prefecture. *Japan Urban Sci* 1:7. <https://doi.org/10.3390/urbansci1010007>
- Rozalis S, Morin E, Yair Y, Price C (2010) Flash flood prediction using an uncalibrated hydrological model and radar rainfall data in a Mediterranean watershed under changing hydrological conditions. *J Hydrol* 394:245–255. <https://doi.org/10.1016/j.jhydrol.2010.03.021>
- Roy S (2011) Flood Hazards in Jalpaiguri District. Unpublished Ph.D. Thesis, Department of Applied Geography, University of North Bengal, Siliguri. <http://ir.nbu.ac.in/handle/123456789/1335>
- Saaty TL (1977) A scaling method for priorities in hierarchical structures. *J Math Psychol* 15:234–281. [https://doi.org/10.1016/0022-2496\(77\)90033-5](https://doi.org/10.1016/0022-2496(77)90033-5)
- Saaty TL (1980) The analytic hierarchy process: planning, priority setting, resource allocation. McGraw-Hill International Book Co, New York, London ISBN: 0070543712 9780070543713
- Saaty TL (1990) How to make a decision: the analytic hierarchy process. *Eur J Oper Res* 48(1):9–26. [https://doi.org/10.1016/0377-2217\(90\)90057-I](https://doi.org/10.1016/0377-2217(90)90057-I)
- Saha AK, Agrawal S (2020) Mapping and assessment of flood risk in Prayagraj district, India: a GIS and remote sensing study. *Nanotechnol Environ Eng* 5:11. <https://doi.org/10.1007/s41204-020-00073-1>
- Samanta S, Koloa C, Kumar Pal D, Palsamanta B (2016) Flood risk analysis in lower part of Markham river based on multi-criteria decision approach (MCDA). *Hydrology* 3(3):29. <https://doi.org/10.3390/hydrology3030029>
- Samanta S, Pal DK, Palsamanta B (2018) Flood susceptibility analysis through remote sensing, GIS and frequency ratio model. *Appl Water Sci* 8:66. <https://doi.org/10.1007/s13201-018-0710-1>
- Sener S, Sener E, Karagüzel R (2011) Solid waste disposal site selection with GIS and AHP methodology: a case study in Senirkent-



- Uluborlu (Isparta) Basin, Turkey. *Environ Monit Assess* 173(1–4): 533–554. <https://doi.org/10.1007/s10661-010-1403-x>
- Sharma S, Roy PS, Chakravarthi V (2017) Flood risk assessment using multicriteria analysis: a case study from Kopili River Basin, Assam, India. *Geomatics Nat Hazards Risk* 9:79–93. <https://doi.org/10.1080/19475705.2017.1408705>
- Shrestha UB, Gautam S, Bawa KS (2012) Widespread climate change in the Himalayas and associated changes in local ecosystems. *PLoS* 7(5):1–10. <https://doi.org/10.1371/journal.pone.0036741>
- Shrestha A, Agrawal N, Alfthan B, Bajracharya SR, Maréchal J, Oort BV (2015) The Himalayan climate and Water Atlas. ICIMOD, Kathmandu Retrieved from: <https://lib.icimod.org/record/31180>
- Smith K, Ward R (1998) Mitigating and managing flood losses. *Floods: Physical Processes and Human Impacts*. John Wiley & Sons, Chichester ISBN: 978-0-471-95248-0
- Starkel L, Sarkar S, Soja R, Prokop P (2008) Present-day evolution of the Sikkimese-Bhutanese Himalayan piedmont. *IGIPZ PAN*, 219. <https://www.rcin.org.pl/igipz/publication/225>
- Souissi D, Zouhri L, Hammami S, Msaddek MH, Zghibi A, Dlala M (2019) GIS based MCDM–AHP modeling for flood susceptibility mapping of arid areas, southeastern Tunisia. *Geocarto Int* 35:991–1017. <https://doi.org/10.1080/10106049.2019.1566405>
- Tang X, Li J, Liu M, Liu W, Hong H (2020) Flood susceptibility assessment based on a novel random Naïve Bayes method: A comparison between different factor discretization methods. *Catena* 190:104536. <https://doi.org/10.1016/j.catena.2020.104536>
- Tapsell SM, Penning-Rowsell EC, Tunstall SM, Wilson TL (2002) Vulnerability to flooding: health and social dimensions. *Phil Trans R Soc A* 360:1511–1525. <https://doi.org/10.1098/rsta.2002.1013>
- Tehrany MS, Pradhan B, Jebur MN (2013) Spatial prediction of flood susceptible areas using rule based decision tree (DT) and a novel ensemble bivariate and multivariate statistical models in GIS. *J Hydrol* 504:69–79. <https://doi.org/10.1016/j.jhydrol.2013.09.034>
- Tehrany MS, Lee MJ, Pradhan B, Jebur MN, Lee S (2014) Flood susceptibility mapping using integrated bivariate and multivariate statistical models. *Environ Earth Sci* 72:4001–4015. <https://doi.org/10.1007/s12665-014-3289-3>
- Tehrany MS, Pradhan B, Jebur MN (2015a) Flood susceptibility analysis and its verification using a novel ensemble support vector machine and frequency ratio method. *Stoch Env Res Risk A* 29(4):1149–1165. <https://doi.org/10.1007/s00477-015-1021-9>
- Tehrany MS, Pradhan B, Mansor S, Ahmad N (2015b) Flood susceptibility assessment using GISbased support vector machine model with different kernel types. *Catena* 125:91–101. <https://doi.org/10.1016/j.catena.2014.10.017>
- Telegraph (2020) Rains trigger floods in three districts. Retrieved from: <https://www.telegraphindia.com/west-bengal/rains-trigger-floods-in-jalpaiguri-alipurduar-and-cooch-behar-districts/cid/1783775>.
- The economic times (2015) 400 people affected by flood in West Bengal's Jalpaiguri district. Retrieved from: <https://economictimes.indiatimes.com/news/politics-and-nation/400-people-affected-by-flood-in-west-bengals-jalpaiguri-district/articleshow/47893460.cms>.
- Vishnu CL, Sajinkumar KS, Oommen T, Coffman RA, Thirvikramji KP, Rani VR, Keerthy RS (2019) Satellite-based assessment of the August 2018 flood in parts of Kerala, India. *Geomatics Nat Hazards Risk* 10:758–767. <https://doi.org/10.1080/19475705.2018.1543212>
- Yalcin A, Reis S, Aydinoglu AC, Yomralioglu T (2011) A GIS-based comparative study of frequency ratio, analytical hierarchy process, bivariate statistics and logistics regression methods for landslide susceptibility mapping in Trabzon, NE Turkey. *Catena* 85(3):274–287. <https://doi.org/10.1016/j.catena.2011.01.014>
- Youssef AM, Pradhan B, Sefry SA (2016) Flash flood susceptibility assessment in Jeddah city (Kingdom of Saudi Arabia) using bivariate and multivariate statistical models. *Environ Earth Sci* 75(1):12. <https://doi.org/10.1007/s12665-015-4830-8>
- Zhao G, Pang B, Xu Z, Yue J, Tu T (2018) Mapping flood susceptibility in mountainous areas on a national scale in China. *Sci Total Environ* 615:1133–1142. <https://doi.org/10.1016/j.scitotenv.2017.10.037>